

## Nuclear Medicine and Early Discovery of Disease

**Presentation by I. C. Baianu,  
FSHN & NPRE Departments, University of Illinois at Urbana,  
URBANA, IL. 61801, USA**

**Two major selected examples:**

- ❖ **Alzheimer's Disease (AD), (affected by Diabetes and Heart Disease)**
- ❖ **Cancer and Early Discovery *via* Molecular Imaging**

# Nuclear Medicine

**Nuclear Medicine** is concerned with applications in **Medicine of Nuclear Science and Engineering techniques and knowledge.**

**On a practical level it involves the use of instruments designed for the detection and location of selected isotopes in the human body for the purpose of medical diagnosis\*.**

**\*Understanding Nuclear Medicine :**

[http://www.youtube.com/watch?v=v\\_8xM-mLxJ8&feature=related](http://www.youtube.com/watch?v=v_8xM-mLxJ8&feature=related)

**What is Nuclear Medicine?      ``SNM's Technologist Section: A Student's Perspective``:**

**``The hottest job around``:** <http://www.youtube.com/watch?v=NcFJbAOgrI8&feature=related>

Understanding PET scans, Alan Waxman, M.D. : SNM Channel 1

<http://www.youtube.com/watch?v=5hHiUleg1IA&feature=relmfu>

# Rationale

- There is an urgent need for the early detection of diseases such as Alzheimer's (AD) and Cancers in order to enable their successful treatment;
- Cancer is the second major cause of death after Heart Disease, and AD is the third major cause of death with **major consequences for the society**
- Three major Nuclear Medicine techniques that are established for diagnostic and research purposes are:
  - Positron Emission Tomography (PET) and CAT/CT
  - Nuclear Magnetic Resonance Imaging (NMRI/ MRI)

## Proportion of Alzheimer and Dementia Caregivers Who Report High or Very High Emotional and Physical Stress Due to Caregiving

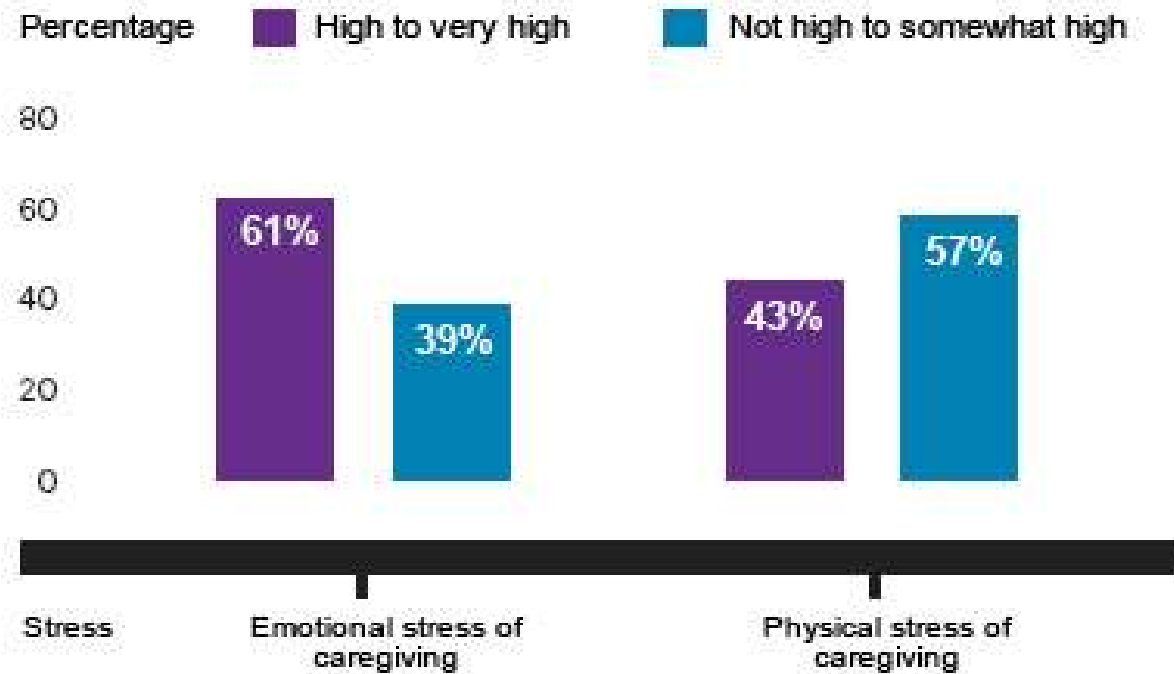


**Figure 1. Social Impact of AD on Caregivers:** There are **15 million** Alzheimer's and dementia caregivers providing 17 billion hours of unpaid care valued at **\$202 billion**; **2030 Projections→\$1 Trillion !** (Bar graph generated from data from the Alzheimer's Association 2010 Women and Alzheimer's Poll, October 2010.)

*Source: Alzheimer's Association 2011 Alzheimer's Disease Facts and Figures.*

## What is Alzheimer's ?

A brain disease that affects a significant fraction of the population over 62-65 years of age by causing problems with short-term memory, thinking, spatial orientation and behavior, worsening over a time span of up to 20 years and in 60 to 80% of cases leading to *dementia*, “a general term for memory loss and other intellectual abilities serious enough to interfere with daily life” (Source: Alzheimer’s org., 2011).

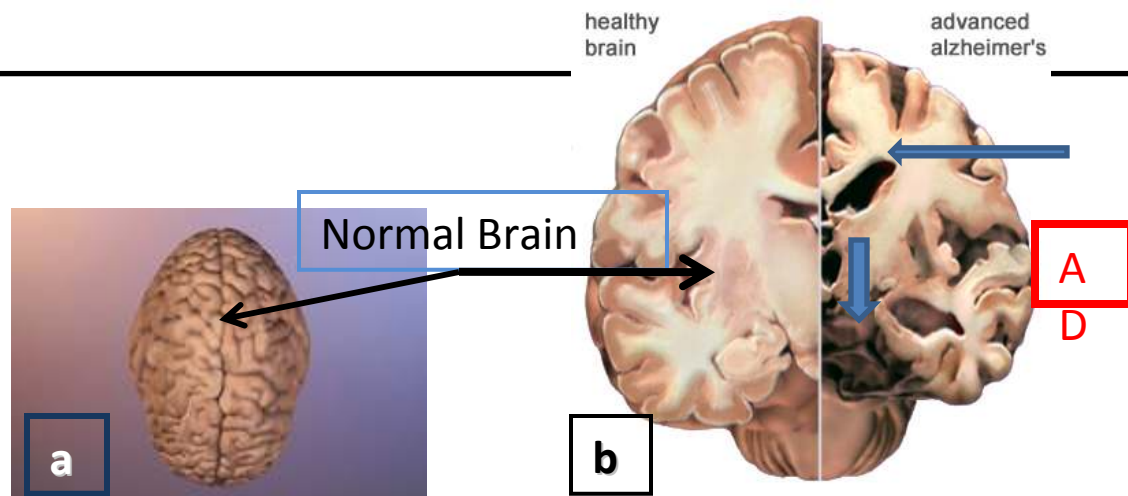


Figure 2.

- a. Normal Human Brain Morphology. b. Comparison between healthy (at left) and advanced **AD** (at right) brains.

## Figure 3. Alzheimer's Early Detection with PET Scans



**Westside Medical Associates of Los Angeles and Westside Medical Imaging (WMI):**  
*“announce the benefit of early **positron emission tomography** (**PET**) scanning to identify Alzheimer's in its **early, more treatable phase.**” (**But, sadly, there is for now no AD treatment !**)*

<http://www.medicexchange.com/PET/alzheimers-early-detection-with-pet-scan.html> Source: *Westside Medical Imaging*

# Positron Emission Tomography (PET)

- **PET is a Nuclear Medicine imaging** technique which generates a 3D-image of the distribution of a positron-emitting **radionuclide tracer** introduced in the human body with a **'marker'** molecule. The PET detectors collect pairs of  $\gamma$ -rays emitted from the positron annihilation with an electron, and scan through the positions of the radionuclide sources from locations within the human body:  $e^+ \leftrightarrow e^- \rightarrow 2 \gamma$  ; example:  $^{18}\text{F}_9 \rightarrow ^{18}\text{O}_8 + \nu + \beta^+$   
(positron: [J. P. Blaser](#), [F. Boehm](#), and [P. Marmier](#) : *Phys. Rev.* (1949) 75:p.1953 "The Positron Decay of  $\text{F}^{18}$  ").
- Images of radionuclide activity distribution in 3-dimensional or 4-D space-time within the body are then reconstructed by fast computers to provide physicians with an image of, for example, the patients brain or the whole body. Recently, scans, such as for 3-D reconstructions are typically refined with the aid of higher resolution, local CT (CAT) scans also performed on the patient simultaneously with the PET scanning.
- "A PET image is a 'photograph' of high-energy  $\gamma$ -rays emitted from a positron-emitting radioisotope. *Several such* short-lived radioisotopes:  $^{18}\text{F}$ ,  $^{11}\text{C}$  and  $^{15}\text{O}$  are made in a cyclotron, and a probe (for example, a drug, or water--*in the case of O-15 of spin 1/2*) is labeled and injected intravenously into a patient. The tracer is imaged in a scanner that comprises a large number of scintillation detectors. The collision of a positron with a nearby electron produces two  $\gamma$ -rays that are separated by 180 degrees. Two scintillation detectors that are separated by 180 degrees transmit a coincident signal when both are stimulated simultaneously. The photon energy that is absorbed by the detectors is re-emitted as visible light and detected by photomultiplier tubes." (*Nature Reviews Cancer*, 4: 457-469 ; June 2004 ). Image resolution is typically 5 to 10mm.

# FDG Marker for PET Imaging

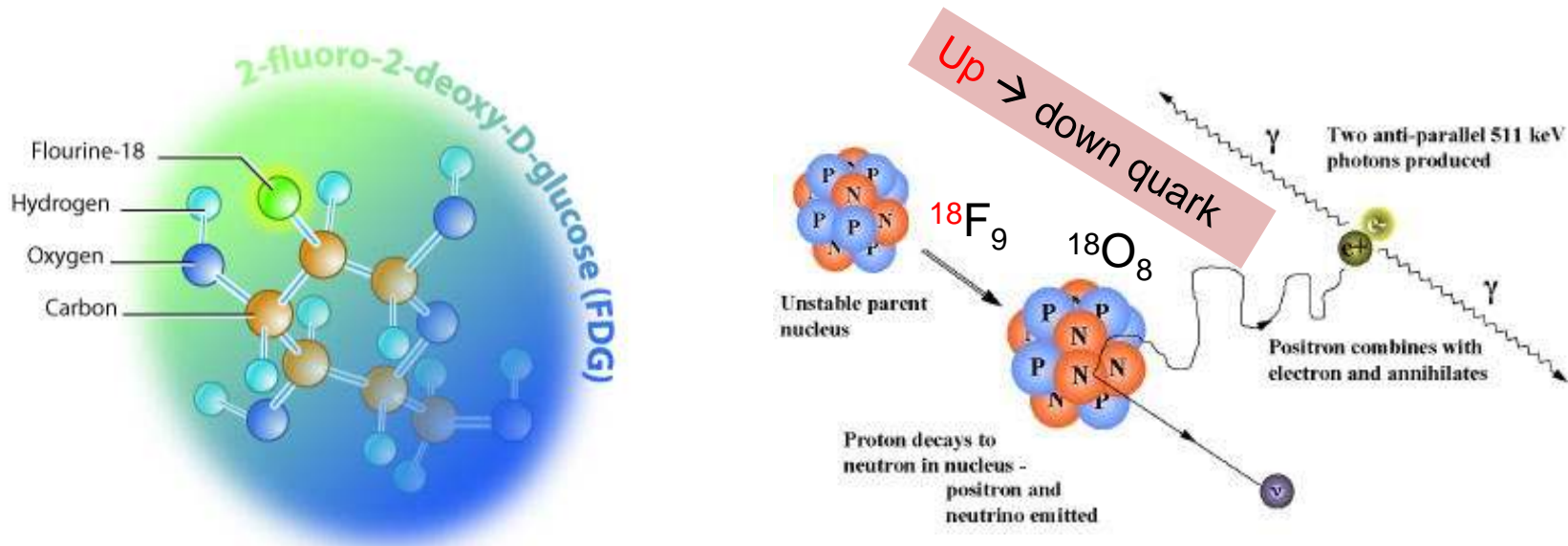


Fig. 4. An example of a PET marker molecule is the analog of 2-deoxy-D-glucose -- Fludeoxyglucose ( $^{18}\text{F}$ ) (IUPAC name 2-Deoxy-2-( $^{18}\text{F}$ ) fluoroglucose)—FDG, which is taken up by the cells in the brain, heart, kidney, liver, etc., where it becomes trapped just like glucose does (through processes involving metabolic phosphorylation)

The equivalent dose absorbed from the injected marker FDG ( $^{18}\text{F}$ -Fluoro deoxyglucose) is typically 8 mSv for adults using 400 MBq for PET imaging-- much lower than whole body CT scans (~30 mSv).

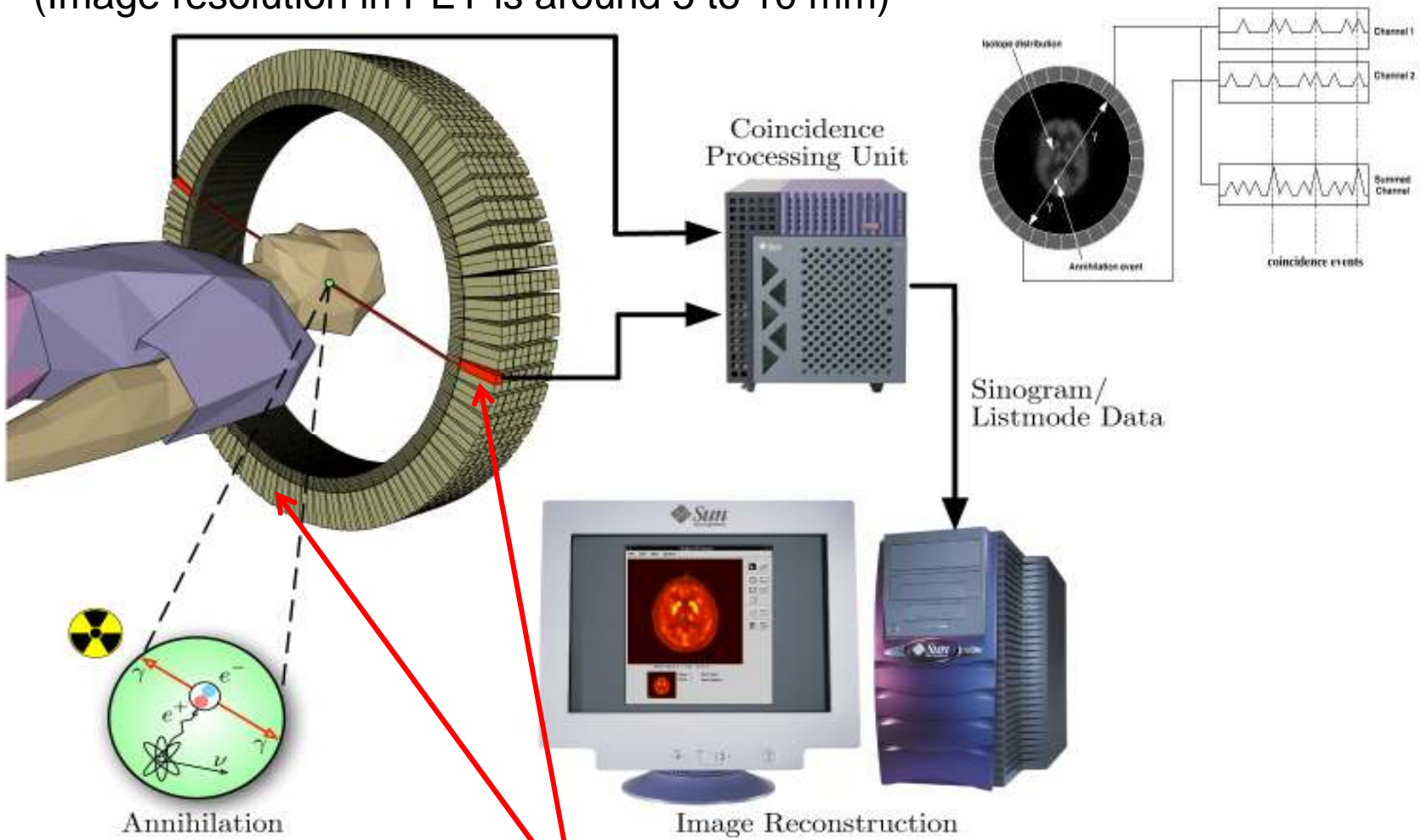
Oxygen-18 ( $^{18}\text{O}$ ) -- a natural, stable isotope of oxygen( $Z=8$ )--is an important precursor for the production of fluorodeoxyglucose (FDG) used in positron emission tomography (PET). In the radiopharmaceutical industry, enriched water ( $\text{H}_2^{18}\text{O}$ ) is bombarded with protons in either a cyclotron or a linear accelerator generating Fluorine-18.  $^{18}\text{F}$  is then synthesized into FDG and injected into a patient. It can also be used to make a heavier version of tritiated water,  $^3\text{H}_2^{18}\text{O}$ ; the radioactive O-18 tritiated water has a density ~30% greater than the abundant water,  $^1\text{H}_2^{16}\text{O}$ . [PET-MIPS-anim.gif](http://upload.wikimedia.org/wikipedia/commons/thumb/3/3d/PET-MIPS-anim.gif/220px-PET-MIPS-anim.gif) :

<http://upload.wikimedia.org/wikipedia/commons/thumb/3/3d/PET-MIPS-anim.gif/220px-PET-MIPS-anim.gif>



# Figure 5a. PET Scanner Principle Diagram

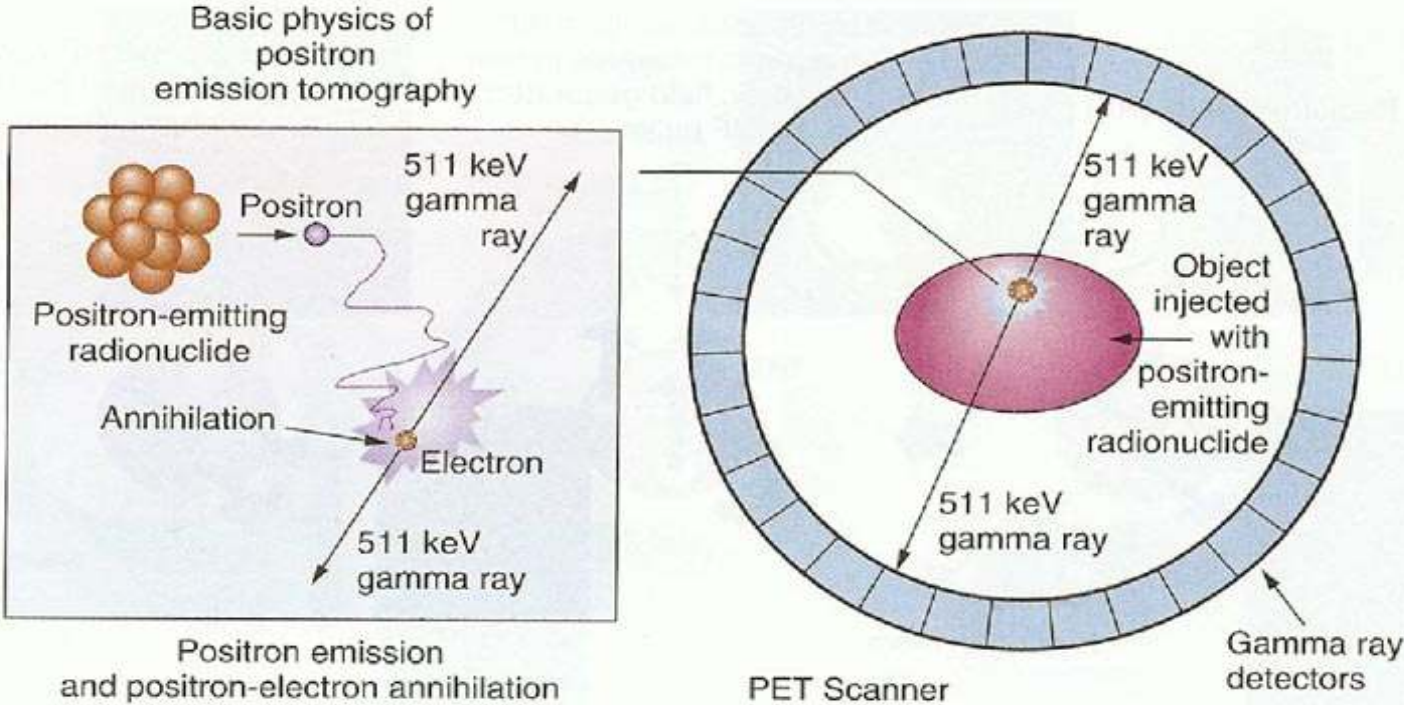
(Image resolution in PET is around 5 to 10 mm)



Source: Diagram courtesy of [Jens Langner](#) Multiple/ distributed  $\gamma$ -detectors.

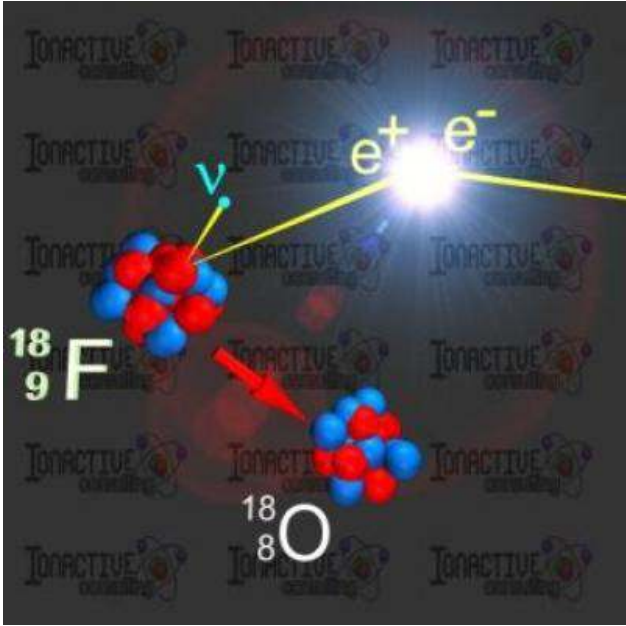
In a PET camera, each detector generates a timed pulse when it registers an incident photon. These pulses are then combined in coincidence circuitry, and if the pulses fall within a very short time-window, they are selected as being coincident.

# Figure 5b. Positron Emission and Annihilation



By collecting millions of events, the PET scanner is able to create an image of the body that demonstrates where the greatest accumulation of labeled glucose is. This image can be then superimposed onto a much higher resolution CAT/CT image ; **Source: <http://cellsighttech.com/technology/pet.html>**

# Figure 5c. Positron Emission and Annihilation Example



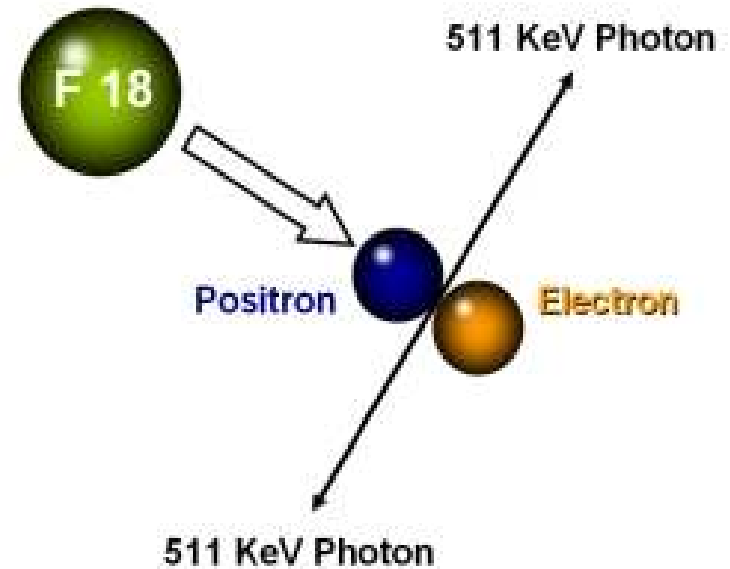
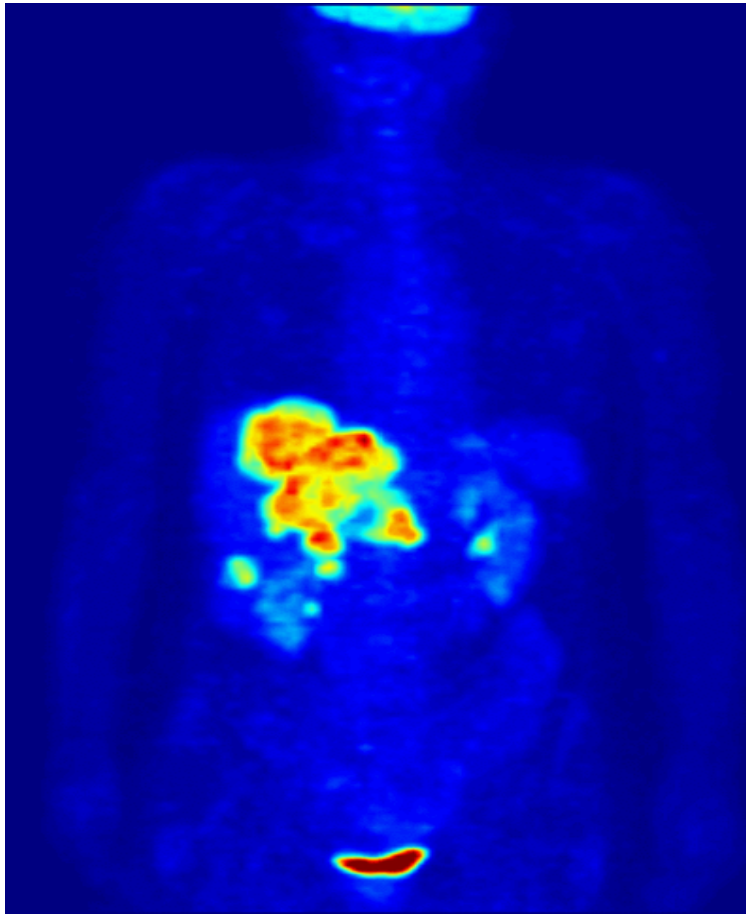


## Figure 6. Whole Body PET Scan Imaged with $^{18}\text{F}$ -FDG.

FDG is taken up by cells like normal glucose. More active cells, such as some cancer and inflammatory cells will take up more FDG than the surrounding tissue; such FDG –rich areas will produce greater numbers of photons, acting like a red ‘beacon’, showing up the abnormal sites. The injection is radioactive, but only for a short time. There are so far no reported side effects to an FDG injection, and no sensation other than the regular injection!

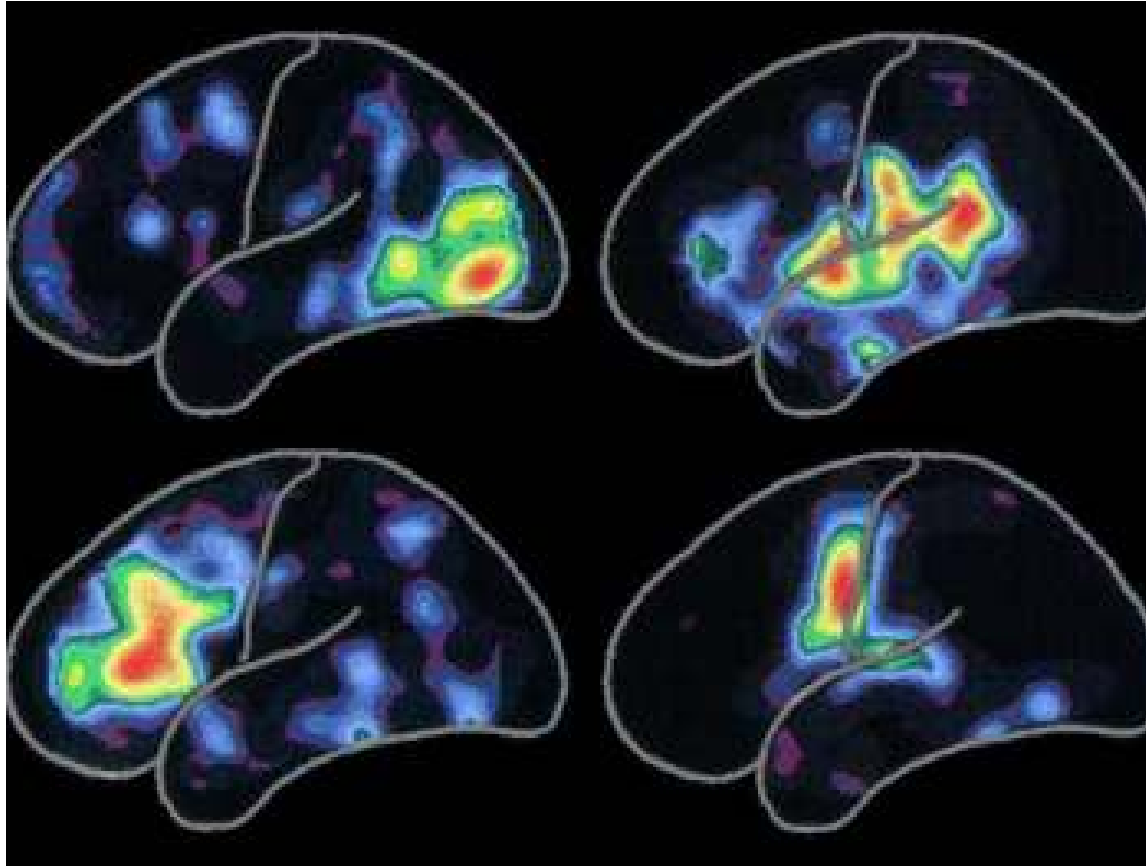


**Figure 7. Positron Emission Tomography (PET)** scans of the normal human brain showing several patterns of brain activity associated with human speech and learning (reading or hearing words): **red** colored areas represent the highest activity zones, whereas **violet** show the least active areas.

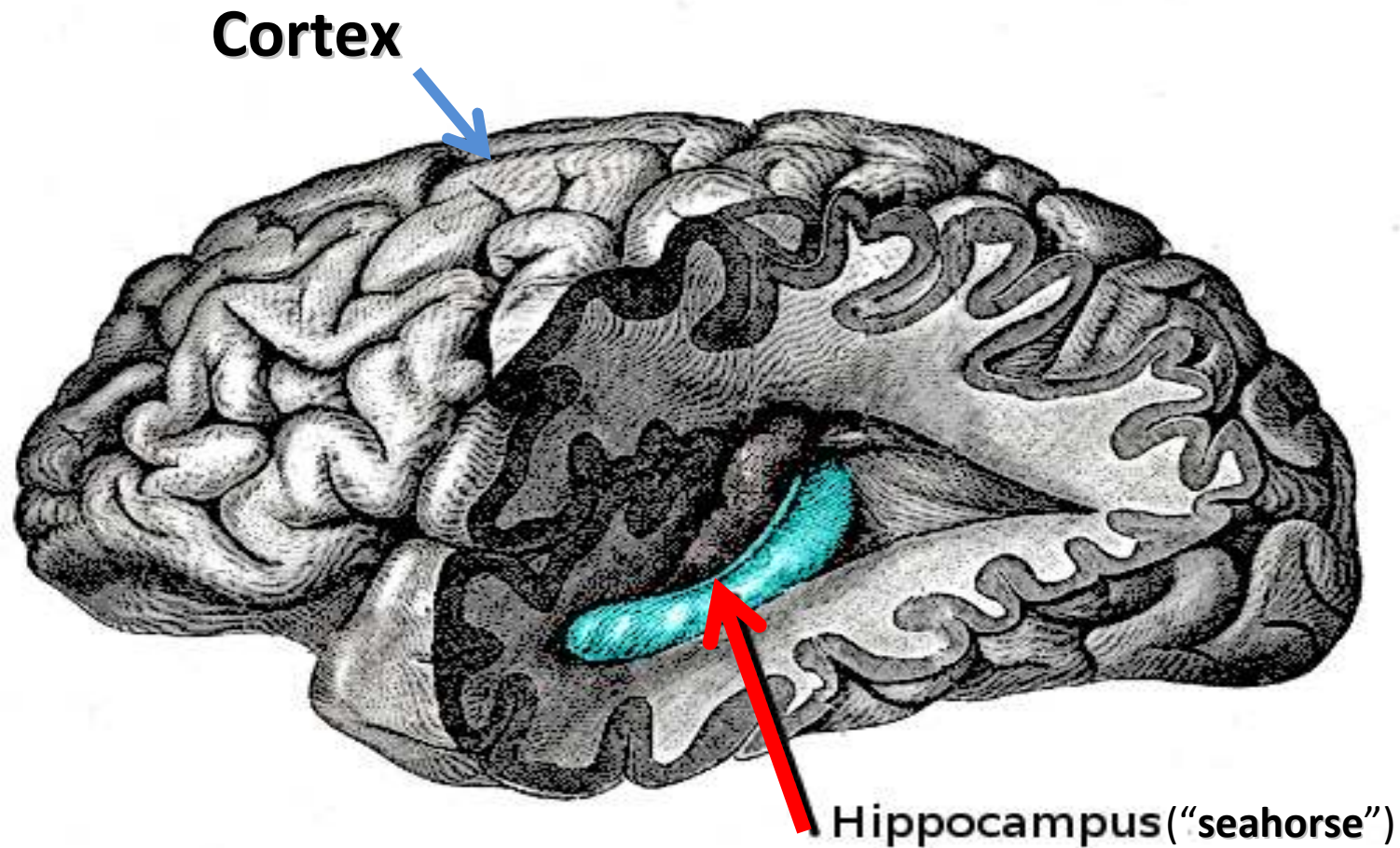


**Figure 8. Drawing of a Human Brain showing the exposed Hippocampus region considered to be involved in short-memory, learning and spatial orientation. Apparently our short-term memory rides on this “seahorse”. There are claims that the Hippocampus is the first zone affected by AD, *but the story appears to be much more complex, as morphological changes are finally spread over the entire cortex.***

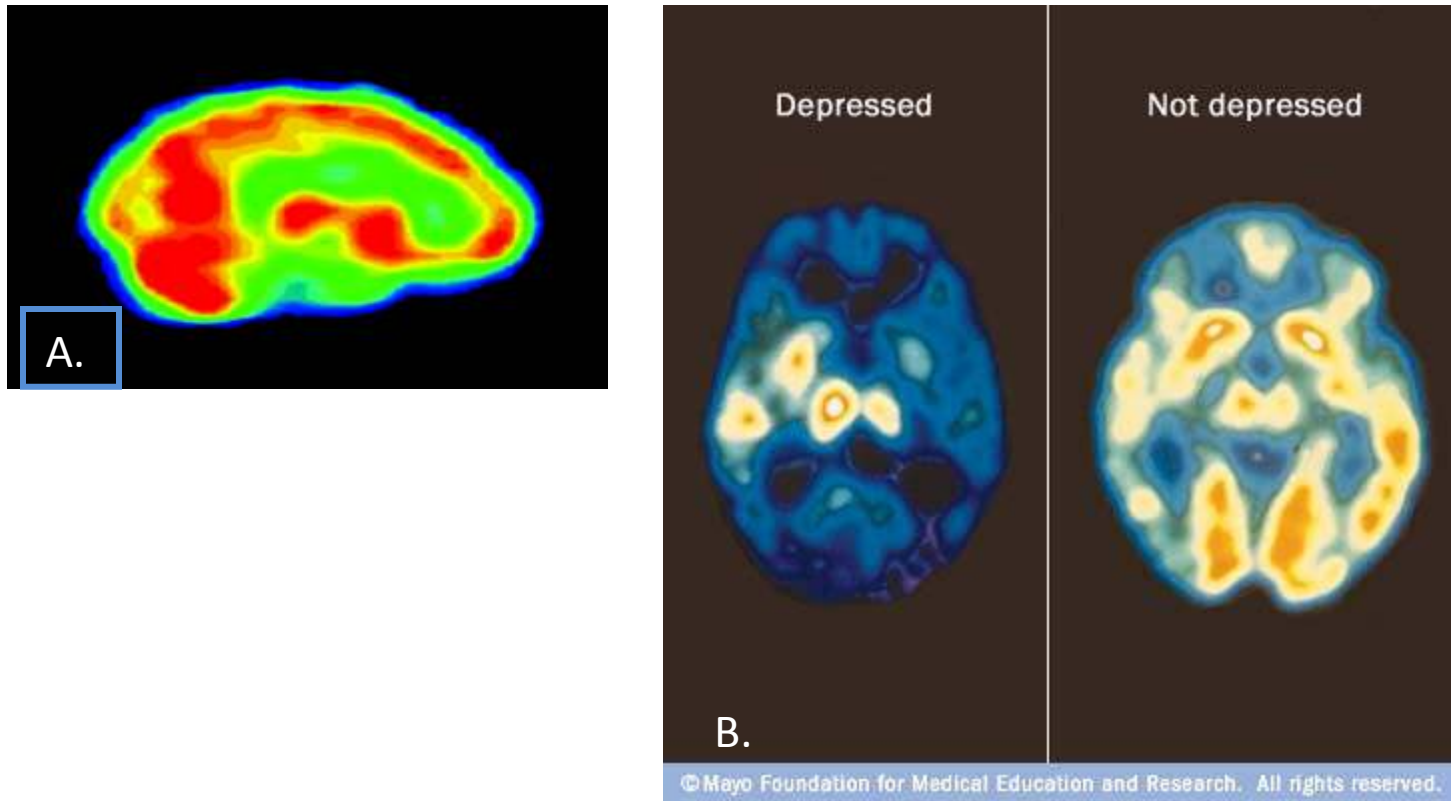
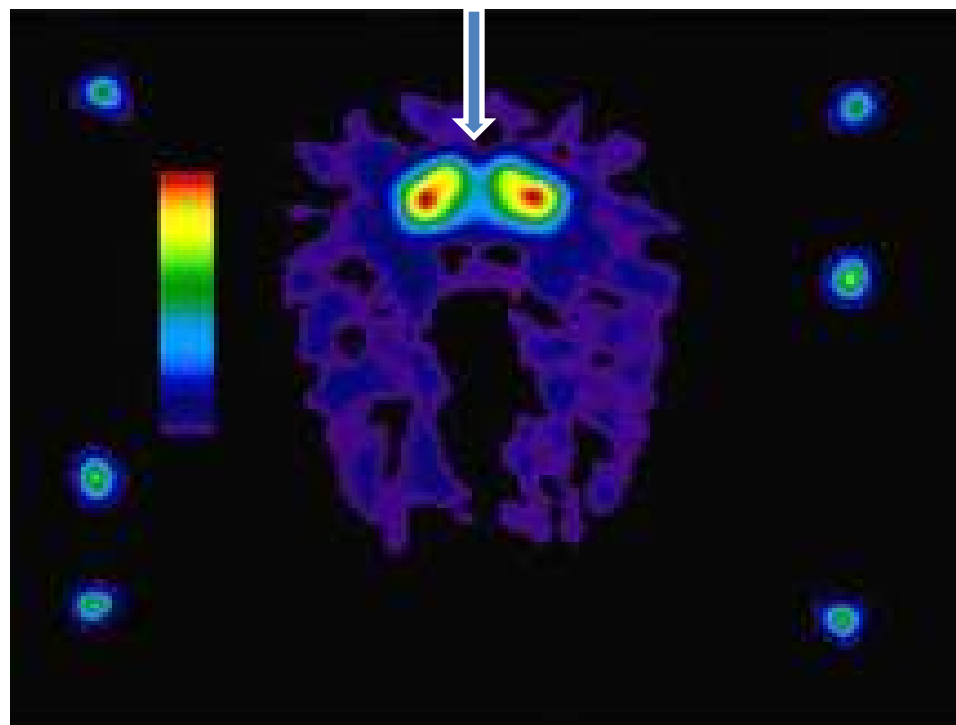


**Figure 9. PET Scan of a Patient's Brain suffering from Depression compared with that of a normal human subject.**

- A. Source : <http://www.physics.utoronto.ca/~key/PHY138/>  
(The Nuclear and Radiation Section of PHY138Y : **Basic Reading Material**)
- B. Source: Mayo Foundation (MF-MER)

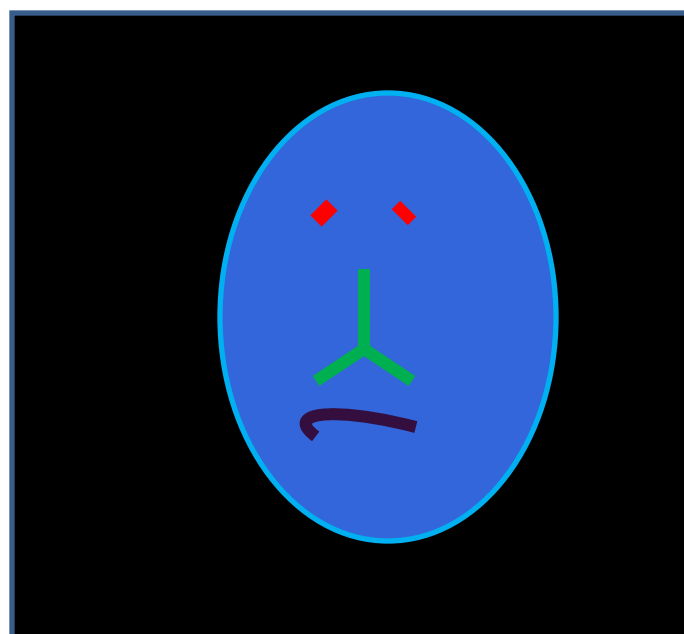
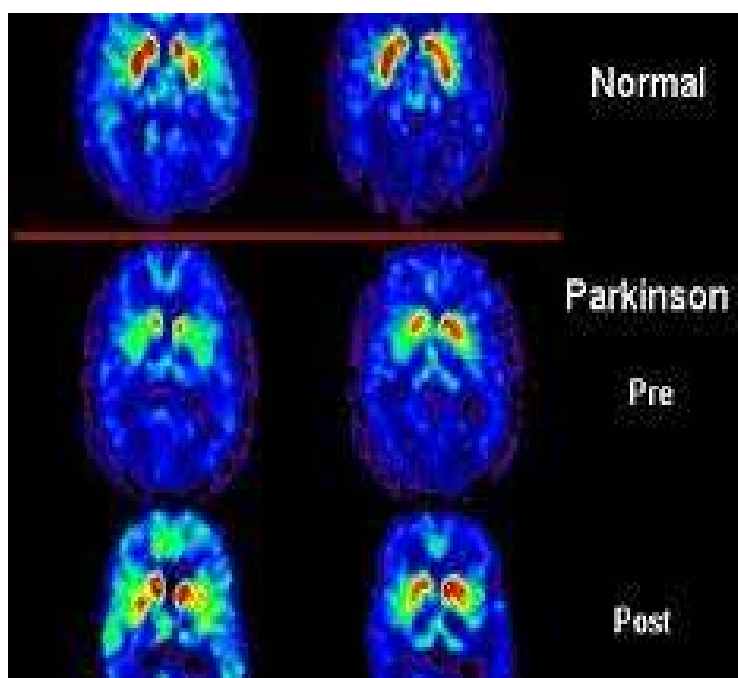
## Figure 10. PET Scan at BNL of a Monkey Brain



*DOE Photo : ``The above PET scan shows the chemical marker uptake in a monkey's brain to test the effectiveness of a Parkinson's disease treatment. The research is being carried out by the Lawrence Berkeley National Laboratory in collaboration with Somatix Therapy Corporation. By restoring levels of important brain chemicals in animals with Parkinson's , the hope is to develop a similar treatment for human patients.'`*



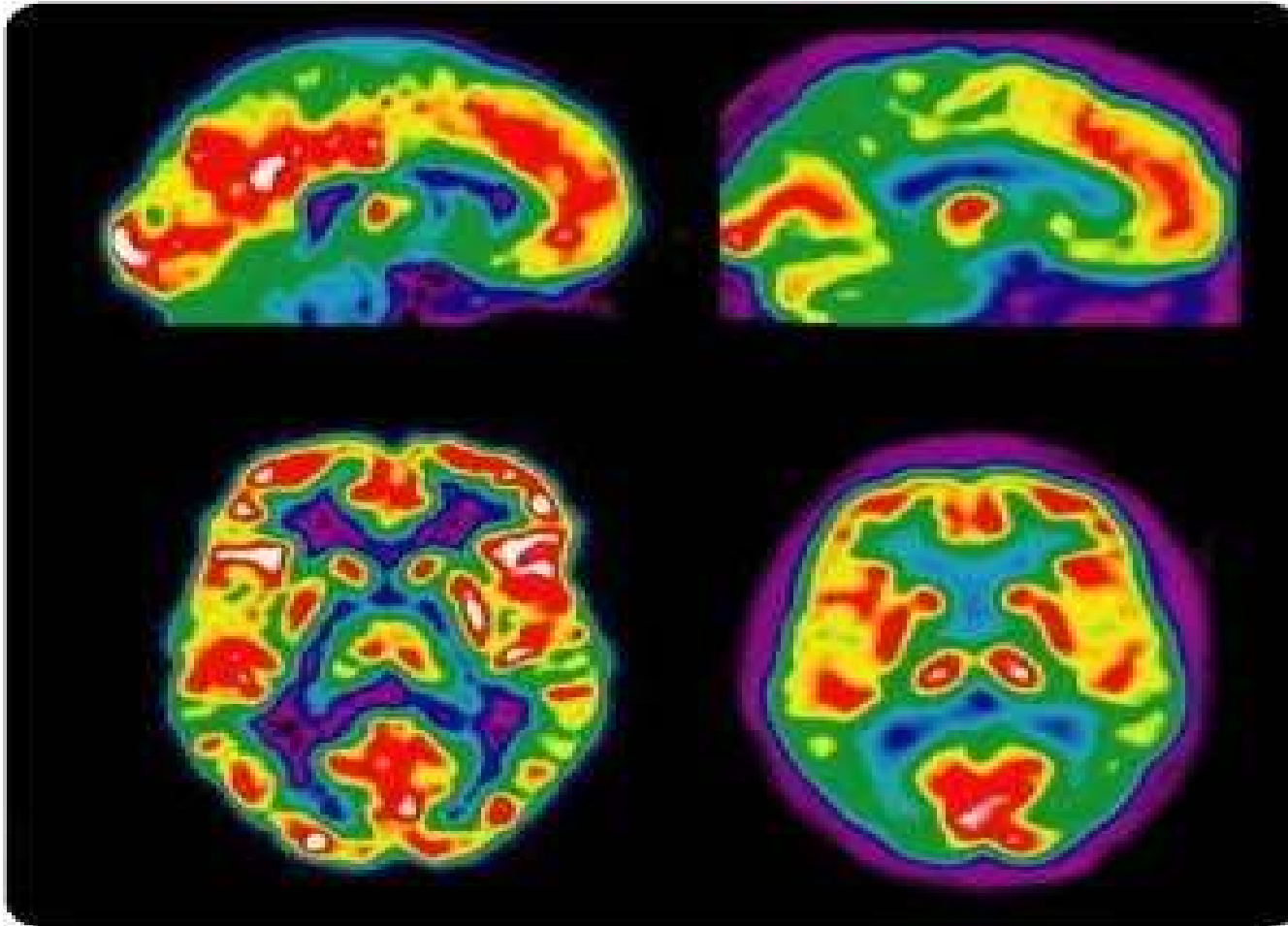
## Figure 11. Example of PET scans for detecting Parkinson's Disease in the Human Brain



The 'sorry' man PET image !

**Note the huge differences between Parkinson's and Alzheimer's PET scan images:** in Parkinson's there is too high a level of neuron excitation—especially certain motor neurons causing tremors, whereas in Alzheimer's one sees the opposite, but at the earlier stages in quite different areas of the brain being affected, *as we shall see more in the following PET scan pictures...*

**Figure 12. Comparisons between, respectively, the sagittal and axial PET-scan images of normal (left) and AD patient's (at right) brains**



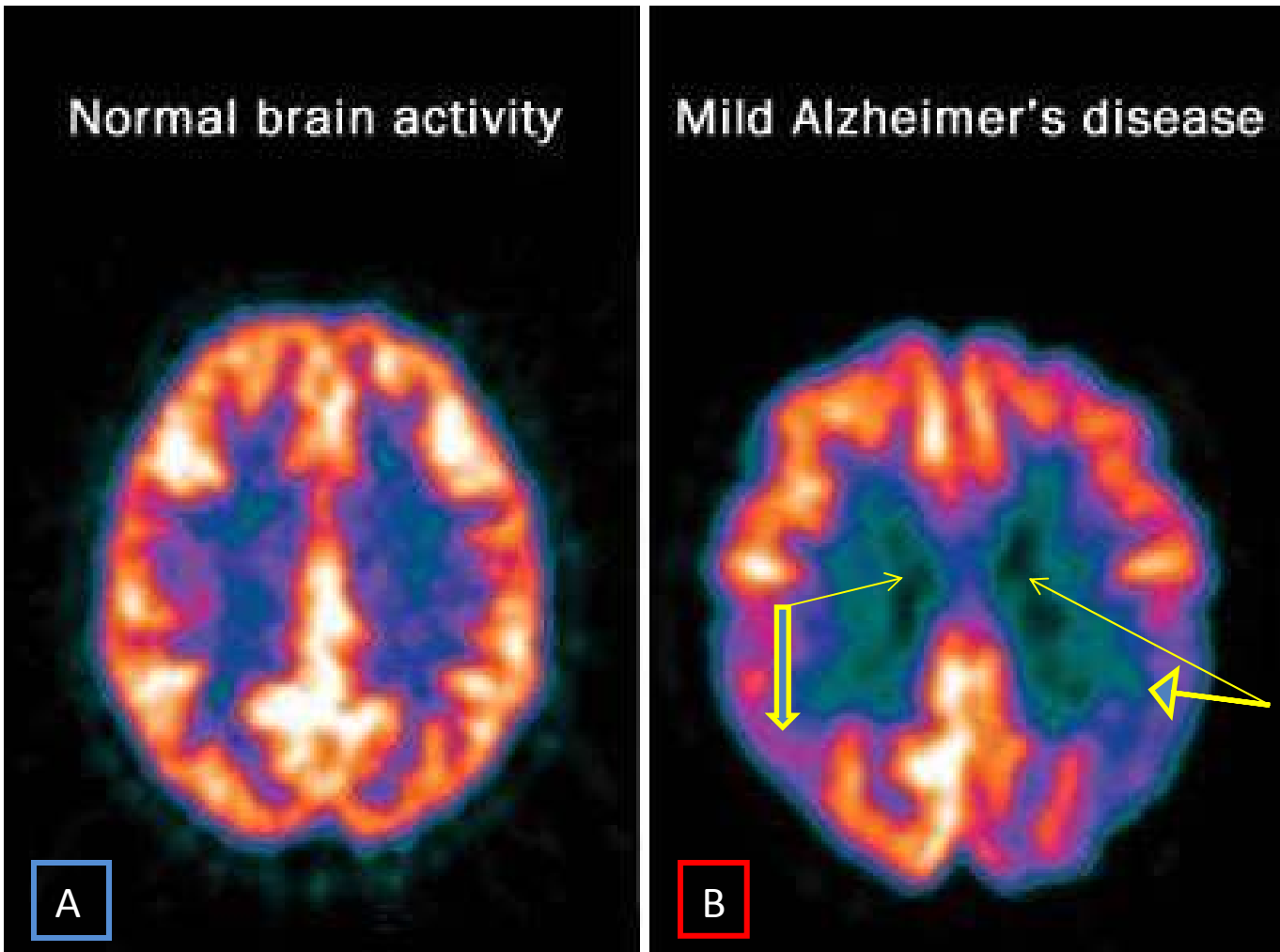


**Figure 13. Comparison between PET Scans of Normal (A) and AD (B) Brains: Note very large differences at arrows.**

3D MRI of human brain:

<http://www.youtube.com/watch?v=XwUn64d5Ddk&feature=related>

# Which Nuclides and Markers can be used for PET/ SPECT detection of AD?

- **FDDNP**: binds to plaques and 'tangle' deposits in the brain
- **PiB= Pittsburgh marker** : claimed to bind specifically to **aggregated  $A\beta$** , and  $^{11}\text{C}$ -labeled biomolecules
- **$^{18}\text{F}$ - in FDG** analogue of glucose for investigating sugar metabolism and diabetes-related risks of AD. (NaF-- Sodium Fluoride for PET Bone Imaging)
- $^{82}\text{Rb}$  (Rubidium-82,  $Z=37$ ) for cardiac PET scanning.

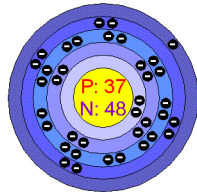


**TABLE 1: Major Isotopes for PET Imaging and Their Medical Applications**

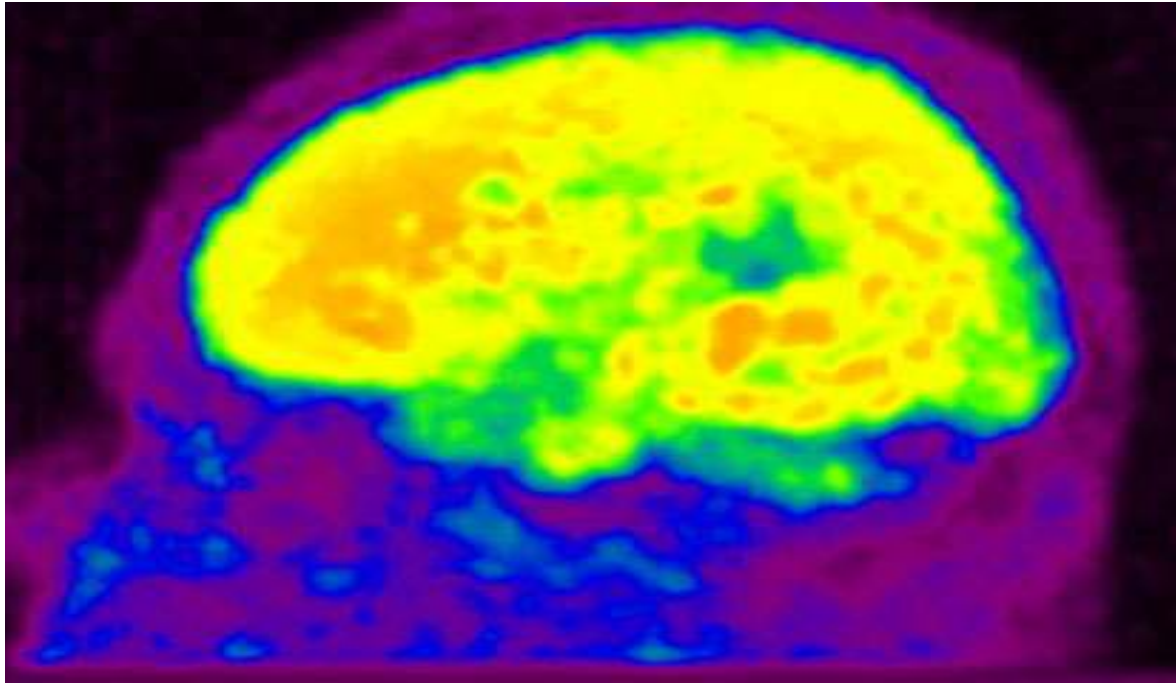
[http://www.schillerinstitute.org/conf-iclc/2007/med\\_isotopes.html#table](http://www.schillerinstitute.org/conf-iclc/2007/med_isotopes.html#table)

<b>Isotope</b>	<b>Half-Life</b>	<b>Diagnostic Applications</b>
Bromine-76	16.0h	Anti-Carcino-embryonic, Antigens, Anti-CEA Antibodies, DNA Studies, Nerves of the Heart, Quantitative Imaging
<b>Carbon-11</b>	<u>20.3m</u>	<b>Diseases:</b> Cancers: Chest, Chronic Lymphocytic, Glioblastoma, Liver, Multiple Myeloma, Prostate, Urinary Tract, <b>Alzheimer's, Brain, Epilepsy, Heart, Parkinson's</b> Alcohol Addiction, Amphetamine Release, Drug Addiction, Neuropsychiatric, Nicotine Dependence, Pain Processing, Schizophrenia, Small Animal Imaging, Tobacco Addiction
Copper-62	<u>9.74m</u>	Cerebral and Myocardial Perfusion, Colorectal Cancer, Human Biodistribution, Liver Cancer, Renal Blood Flow, Renal Injury
Copper-64	12.70h	Cancers: Cervical, Colon, Colorectal, Lymphoma, Melanoma, Pancreatic, Prostate Diseases: Angiogeneses, Brain, Hypoxia, Parkinson's, Wilson's diseases,; Stem Cell Research
<b>Fluorine-18</b>	<b>1.83h</b>	Cancers: Adrenal Gland, Anal, Bone, Bone Marrow Transplants, Bowel, Breast, Cervical, Chest, Colorectal, Esophageal, Gastric, Head & Neck, Hodgkins Disease, Laryngeal, Leukemia, Liver, Lung (NSCLC), Lung(SCLC), Melanoma, Multiple Myeloma, non-Hodgkin's Lymphoma, Osseous, Ovarian, Pancreatic, Prostate, Rectal, Rhabdomjo Sarcoma, Squamous Cell, Thyroid, Urinary, Vocal Cord Diseases: Alcohol Addiction, <b>Alzheimer's Disease, Dementia (as <sup>18</sup>F-FDG)</b> Anorexia, Athersoclerosis, Brain, Depression, Diabetes, Heart, Herpes, HIV, Hypoxia, Infection, Liver, Muscle, Kennedy, Narcolepsy, Lung Inflammation, Osteomyelitin, <b>Parkinson's</b> , Pneumonia, Ulcerative Colitis, Schizophrenia, Tourettes Syndrome, Infection: Pen-Prosthetic, Hip-Prosthetic, Joint-Prosthetic, Small Animal Imaging, Chemotherapy Research

# Table 1B: Other Radionuclides for PET Imaging

- **Gallium-68** : 1.13h
- Breast Cancer, Heart Imaging, **Immunoscintigraphy**, **Molecular Imaging**, Neuroendocrine Tumors, Pancreatic Cancer, **Alzheimer's ?**
- **Iodine-124**: 4.18d
- Apoptosis, Cancer Biotherapy, **Gliomas**, Heart Disease, Mediastinal Micrometastases, Scouting of Therapeutic Radioimmunoconjugates, Thyroid Cancer, **Alzheimer's ?**
- **Iron-52** : 8.28h
- Anemia, Human Bone Marrow
- **Nitrogen-13**: 9.97m
- Ammonia Dog Studies, **Coronary Artery Disease**, **Diabetes**, Gamma Camera, Heart Disease, Imaging of Heart, Pancreas and Liver, Lupus Erythematosus, Myocardial Perfusion, Pulmonary Ventilation
- **Oxygen-15** 122.s
- **Acute Brain Injury**, Arterial Blood Flow, Brain Cancer, Oxygen Utilization, Brain Studies, Cerebral Blood Volume, Cerebral Responses, Coronary Artery Vasospasm, Coronary Reserve, Heart Disease, **Ischemic Stroke Disease**, Kinetics of Oxygen, Liver Cancer, Myocardial Viability, Oxygen Metabolism, Pain Control, Venous Ulceration, **Alzheimer's ?**
- **Rubidium-82**: 1.26m
- Heart Disease, Myocardial Perfusion, Sarcoidosis, **Alzheimer's ?**
- **Yttrium-86** : 14.74h
- Distribution of Y90, Lung Cancer, Melanoma, Renal Cell Carcinoma
- **Zirconium-89**: 3.27d
- Brain Tumors, Head and Neck Cancers, non-Hodgkin's Lymphoma, **Alzheimer's ?**

**Figure 14.** PiB-PET scan of a patient with Alzheimer's Disease.



According to Dr. Elliot Kolin, lead radiologist at WMI: "*the NYU research team used PiB-PET with a fluorescent imaging agent called **Pittsburgh Compound B** that lights up **clumps** of a protein called beta amyloid (A- $\beta$ ) that **are** a characteristic finding of Alzheimer's disease.*" **Normal A- $\beta$  protein does not clump!**

Note the presence of **modified A- $\beta$  clumps**, or hydrophobic **plaques**, also in the frontal areas of the AD brain (*most probably advanced AD*;

Photo Source : Associate Professor Christopher Rowe.

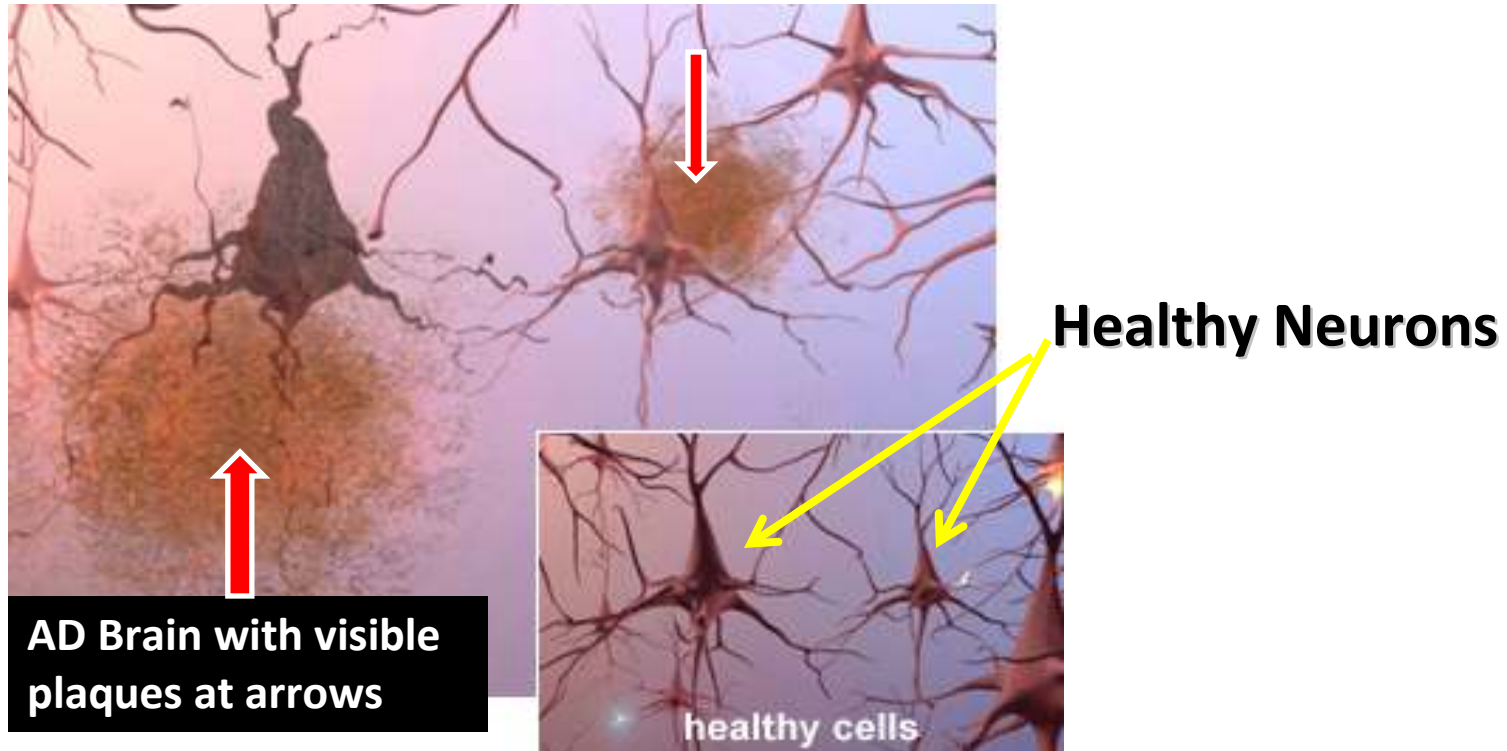
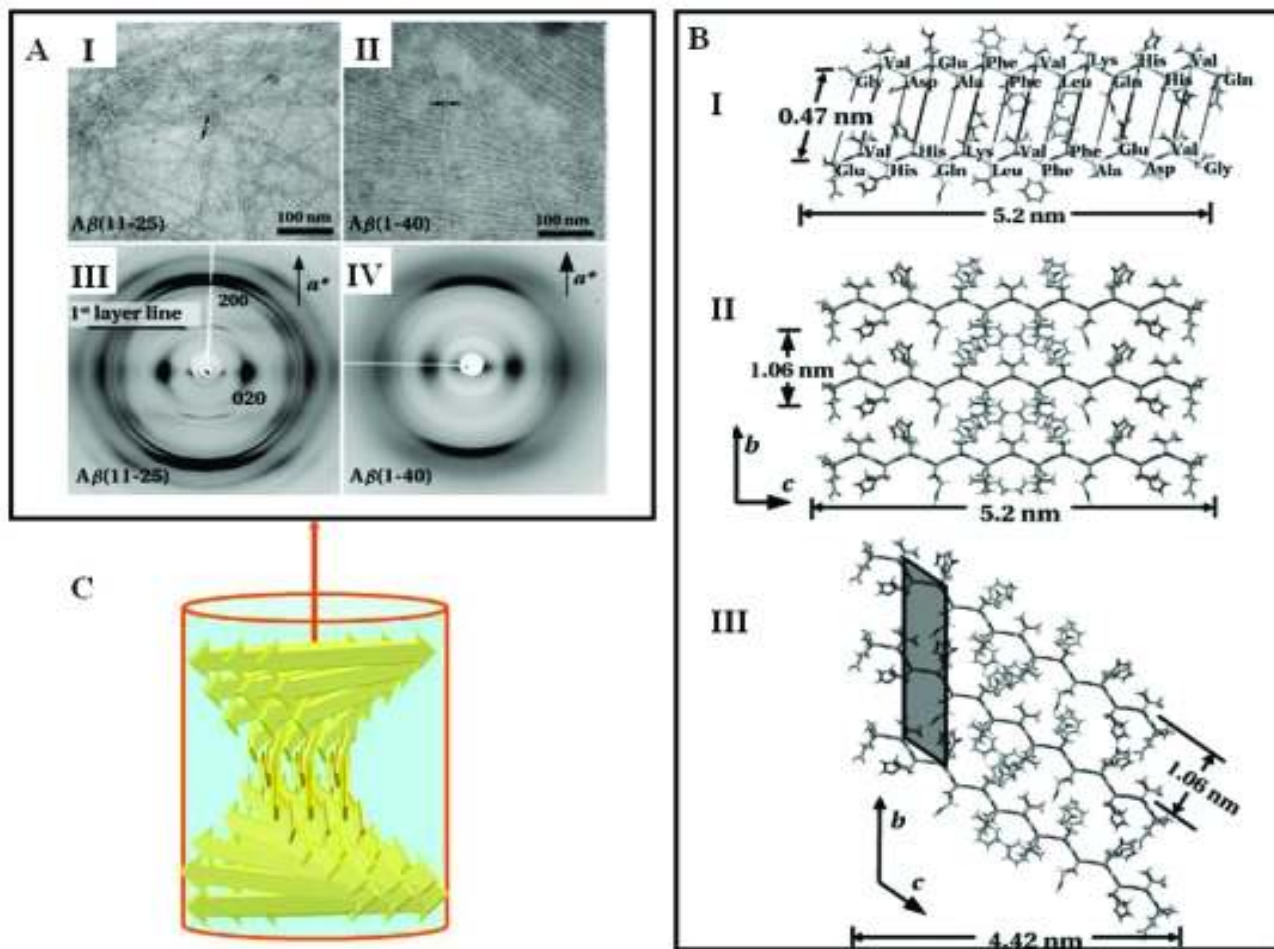


**Figure 15. Microscopic changes of the neurons in the cortex of AD brains compared with those of the normal brain: the orange regions at arrows are modified A- $\beta$  clumps/plaques and/or 'tangles' characteristic of AD. Such microscopic evidence is at present the only medically accepted (post-mortem) confirmation of the AD diagnosis.**



# [Chem Rev. 2010 August 11; 110\(8\): 4820–4838.](#)

**A.** TEM and X-Ray Diffraction (XRD); **B. Models** of  $A\beta_{11-25}$ : I-antiparallel; II. Direct stacking



(A) EM images and X-ray diffraction patterns of cross- $\beta$  ribbons for  $A\beta_{11-25}$  (I) and (III) and  $A\beta_{1-40}$  (II) and (IV). The measured widths of the fibrils are  $\square$ 5 nm for  $A\beta_{11-25}$  and  $\square$ 7 nm for  $A\beta_{1-40}$  (see arrows in I and II).

(C) Illustration of cross- $\beta$  arrangement in amyloids; the peptide backbone  $\beta$ -strands are perpendicular to the fibril axis (arrow).

Source: [Miller Y](#), [Ma B](#), [Nussinov R](#). (2010) & Sikorski et al *Structure*. 2003 Aug;11(8): 915-26.

**PiB** = Pittsburgh compound B = a fluorescent analog of thioflavin T utilized in PET imaging of  $\beta$ -amyloid plaques

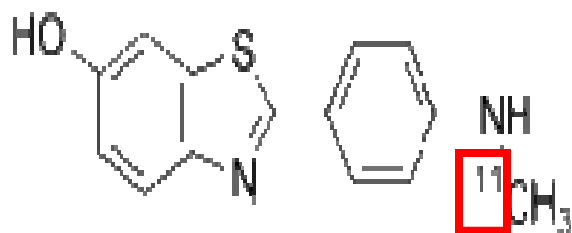
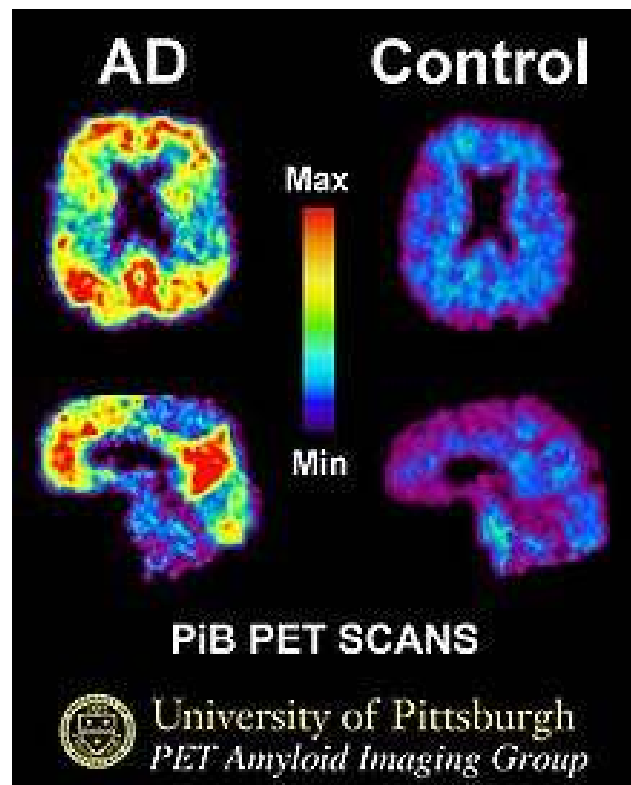


Figure 16. “Areas of **red** and **yellow** show high concentrations of PiB in the brain and suggest **high amounts of  $\beta$ -amyloid deposits in these areas.**”

**Source:** First PET scans on February, 2002, at *Uppsala University*. *Annals Neurology*, 2004



IUPAC name:

[N-Methyl- $^{11}\text{C}$ ]<sub>2</sub>-(4'-methylaminophenyl)-6-hydroxybenzothiazole

# PiB-PET is claimed to detect structural changes associated with AD !

- 1. This is quite important because-- if it is firmly established for all AD type-- it may lead to some progress in understanding the disease, and perhaps also other kinds of dementia, hopefully leading to some treatments **not at all available today!**
- 2. When combined with other types of PET scans it is hoped to link such structural changes with **functional** ones as well, and possibly correlate with AD-related cognitive impairment, such as the learning disabilities of AD patients related to short-term memory loss.
- 3. It has been proposed based on genetic evidence from rare cases of AD--which are **inherited**-- that a specific gene (**ApoE**) and its **ε4** allele are involved:  
Basun, H., Grut, M., Winblad, B. & Lannfeldt, L. (1995). Apolipoprotein **ε4** allele and disease progression in patients with late onset Alzheimer's disease. *Neuroscience Letters*, **183**, 32-34;  
*cited in*: A. S. Macdonald and D. J. Pritchard, 2000).
- This raises the possibility/question if in those AD cases that are not inherited **a genetic mutation (activation of ε4 ??) in ApoE- The Apolipoprotein E Gene-- might occur which would be perhaps induced through either metabolic or environmental factors ?**

# PiB-PET related Publications:

Year	Title	Summary	Authors	Journal
2004	Imaging Brain Amyloid in Alzheimer's Disease with Pittsburgh Compound-B	Retention of [C-11]PiB shown to be approximately 2-fold greater in cortical areas of AD subjects relative to controls. Pattern of retention mirrors the pattern of amyloid deposition known from post-mortem studies.	Klunk, W.E., H. Engler, A. Nordberg, Y. Wang, G. Blomqvist, D.P. Holt, M. Bergstrom, I. Savitcheva, G.F. Huang, S. Estrada, B. Ausen, M.L. Debnath, J. Barletta, J.C. Price, J. Sandell, B.J. Lopresti, A. Wall, P. Koivisto, G. Antoni, C.A. Mathis, and B. Langstrom	Ann. Neurol. <b>55</b> : 306-319
2005	<b>Kinetic Modeling</b> of Amyloid Binding in Humans using PET Imaging and Pittsburgh Compound-B.	Methodology paper describing appropriate methods for the <b>quantification of PiB-PET brain scans.</b> <b>First report using PiB in subjects categorized with mild cognitive impairment (MCI).</b>	Price, J.C., W.E. Klunk, B.J. Lopresti, X. Lu, J.A. Hoge, S.K. Ziolko, D.P. Holt, C.C. Meltzer, <a href="#">S.T. DeKosky</a> , and C.A. Mathis	J Cereb. Blood Flow Metab. <b>25</b> : 1528-1547.

1. Klunk, W.E., et al. 2004. **Imaging brain amyloid in Alzheimer's disease with Pittsburgh Compound-B, *Annals of Neurology*, 2004. 55(3): 306-319.**

2. Kolata, Gina. 2010. ["Promise Seen for Detection of Alzheimer's"](#), *The New York Times* (June 23rd, 2010).

# AD Pathology and Medical Diagnosis

AD Pathology is characterized at least by the following:

- “(a) **senile plaques** (deposits on the outside of neurons , consisting largely of the modified protein  $\beta$ -amyloid)—the adopted post-mortem criterion for confirming the diagnosis of AD;
- (b) amyloid angiopathy (deposits of amyloid protein in the arteries of the brain);
- (c) neurofibrillary ‘tangles’ (dysfunctional connections between neurons);
- (d) **loss of neurons**;
- (e) decreased activity of choline acetyltransferase (an enzyme...involved in *synaptic transmission*)”;
- (f) mutations in two genes labeled presenilin-1 (PS-1) and presenilin-2 (PS-2), which appear to be associated with AD, though the mechanisms remain unclear. (*loc.cit.*)

# The Apolipoprotein E (ApoE) gene involvement in AD

- “The ApoE  $\epsilon 4$  allele has been found to confer risk for AD in a dose related fashion, such that  $\epsilon 4$  homozygotes ( $\epsilon 4 / \epsilon 4$ ) are at a greater risk than  $\epsilon 4$  heterozygotes ( $\epsilon 2 / \epsilon 4$ ,  $\epsilon 3 / \epsilon 4$ ), who in turn are at greater risk than those without the  $\epsilon 4$  allele:”

(Bickeboller et al., 1997; Corder et al., 1994; van Duijn et al., 1995; Farrer et al., 1997; Jarvik et al., 1996; Kuusisto et al., 1994; Lehtovirta et al., 1995; Mayeux et al., 1993; Myers et al., 1996; Poirier et al., 1993; Tsai et al., 1994).

- Some studies have observed that the risk depends on age; ApoE  $\epsilon 4$  seems to have greatest effect at ages 60 to 70, tapering off at older ages: Bickeboller et al., 1997; Corder et al., 1994; Farrer et al., 1997.
- (d) It is also possible that the ApoE  $\epsilon 4$  allele is associated with an earlier onset of AD (not to be confused with the early-onset AD type—which is inherited, in rare cases, i.e.,  $\epsilon 4$  homozygotes:  $\epsilon 4 / \epsilon 4$ ).

# The Modified $\tau$ -Protein in AD

- Another hypothesis about AD causes-- that has gained momentum-- is the involvement of a **modified**/ shortened tau ( $\tau$ )—proteins that normally act as spacers between microtubules in the nutrient transport system of the nerve cells; it has been claimed that the modified  $\tau$ —proteins **aggregate** thus causing the early onset of AD by `messing up' the nutrient transport system of the nerve cells that die later for lack of sufficient nutrients.
- Moreover, it has been claimed that the **A $\beta$**  plaques appear only at later stages of AD, and also that **modified  $\tau$ 's** are a better indicator than **A $\beta$**  plaques for early diagnosis of AD.

# New Strategies:

I. **Combining** Techniques PET/CAT, MRI-NMRI/PET, MRI/CAT,...and Modeling



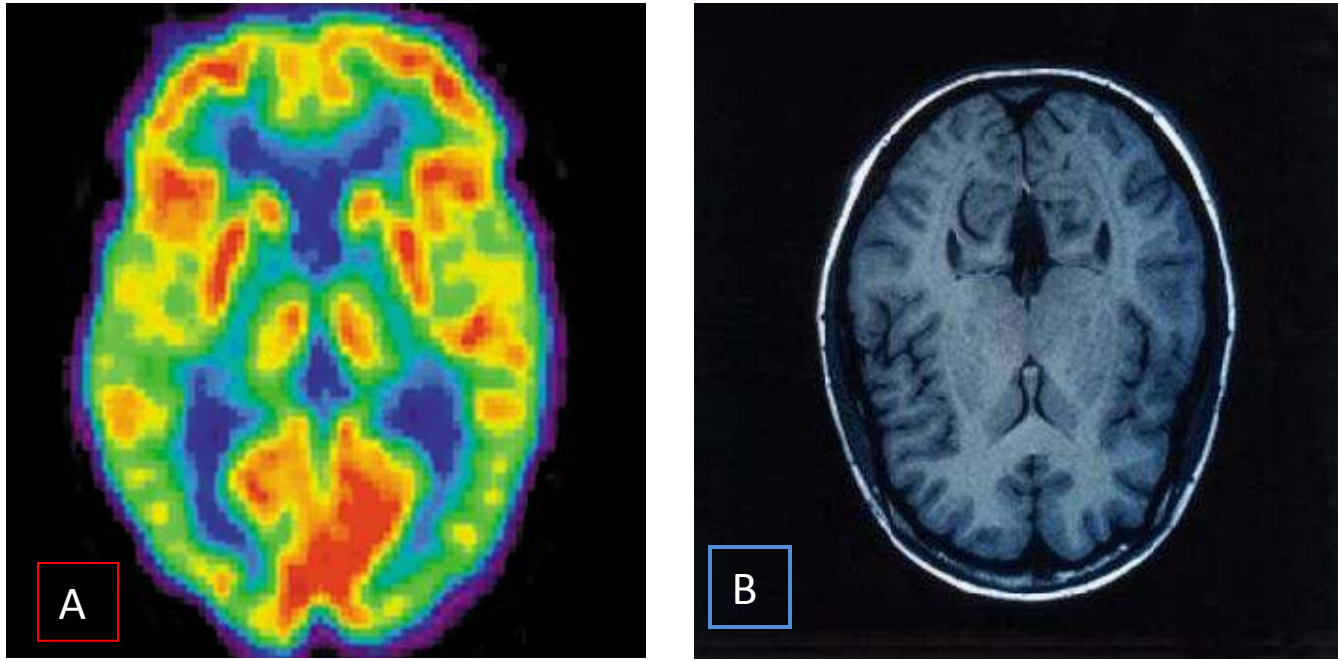


**Figure 17. A. Left: PET Scan of a healthy human brain= SPECT/PET (single photon /positron emission computed tomography):**

**Step 1.** Radio-labeled compounds are injected in tracer amounts

**Step.2.** Their photon emissions can be detected , like X-rays in **CAT** scans. **PET** images made represent the accumulation of the labeled compound; such compounds may reflect **blood flow**, oxygen levels, glucose metabolism, or dopamine transporter concentration –**depending on the radio-labeled tracer**;

**B. at right: MRI Scan of a normal human brain.**

# Comparison of PET Scans of a Healthy Volunteer and Early-Stage AD Human Brains, registered with MRI Images of Healthy Brain

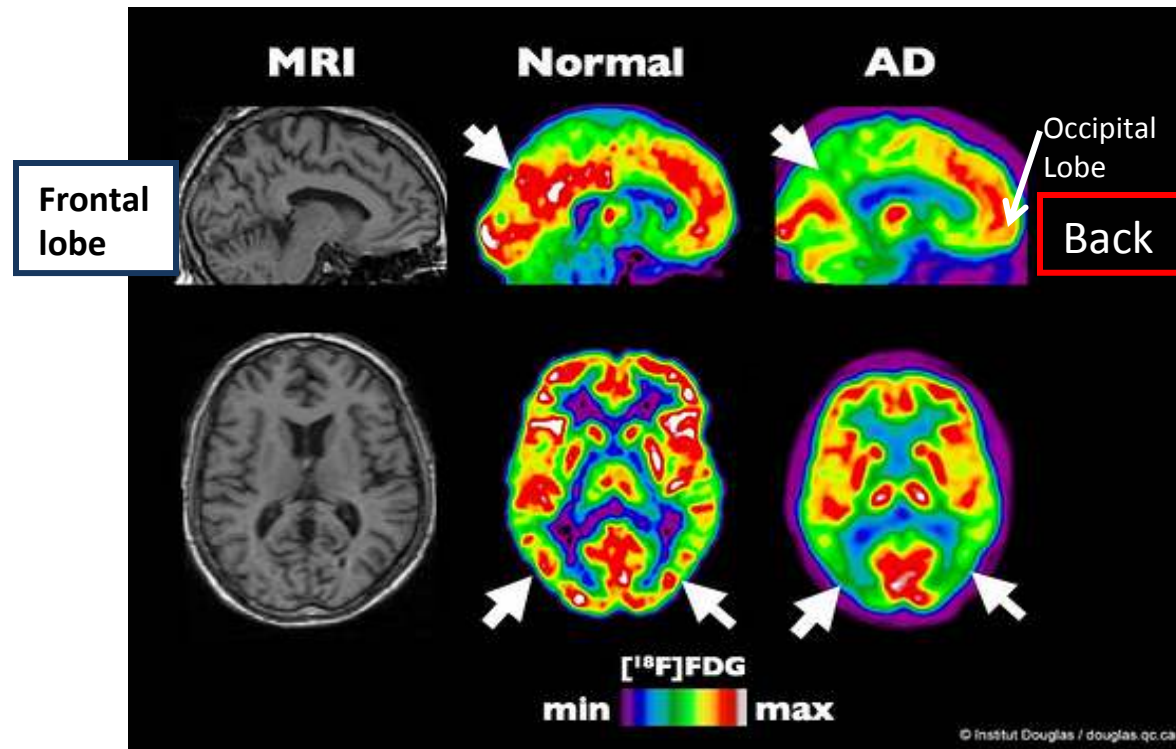


**Figure 18.** In the above PET images red coloring represents the maximum FDG rate of glucose-analog utilization in the human brains and violet the lowest.

The arrows show the posterior temporal-parietal junction (lower row) and the posterior *cingulate gyrus* (top row). Source: <http://www.flickr.com/photos/institut-douglas/2677257668/> Brain Anatomy and Functions: <http://www.youtube.com/watch?v=HVGIfcP3ATI&NR=1>

## Figure 19. PET/CAT Based True Whole-body Field View for Cancer Treatment



*“The study, performed at Saint Louis University in St. Louis, MO, included 500 patients who underwent true whole-body FDG PET/ CAT, from the top of the skull to the bottom of the feet. **59 of 500 patients had PET/ CAT\* findings suggestive of malignancy outside the limited whole-body field of view. **New cancerous involvement was confirmed in 20 of those patients.**”***

**Source:** <http://www.medicexchange.com/PET/petct-based-true-whole-body-field-view-for-cancer-treatment.html>

\* **CAT/CT = Computer Assisted Tomography; CT-scan X-radiation doses: 7 mSv to 30 mSv (“high”).**

# MRI-PET Scanner Combination:

Two kinds of body imaging -- Positron Emission Tomography (PET) and Nuclear Magnetic Resonance imaging (MRI/NMRI) – *“have been combined for the first time in a single scanner”*.

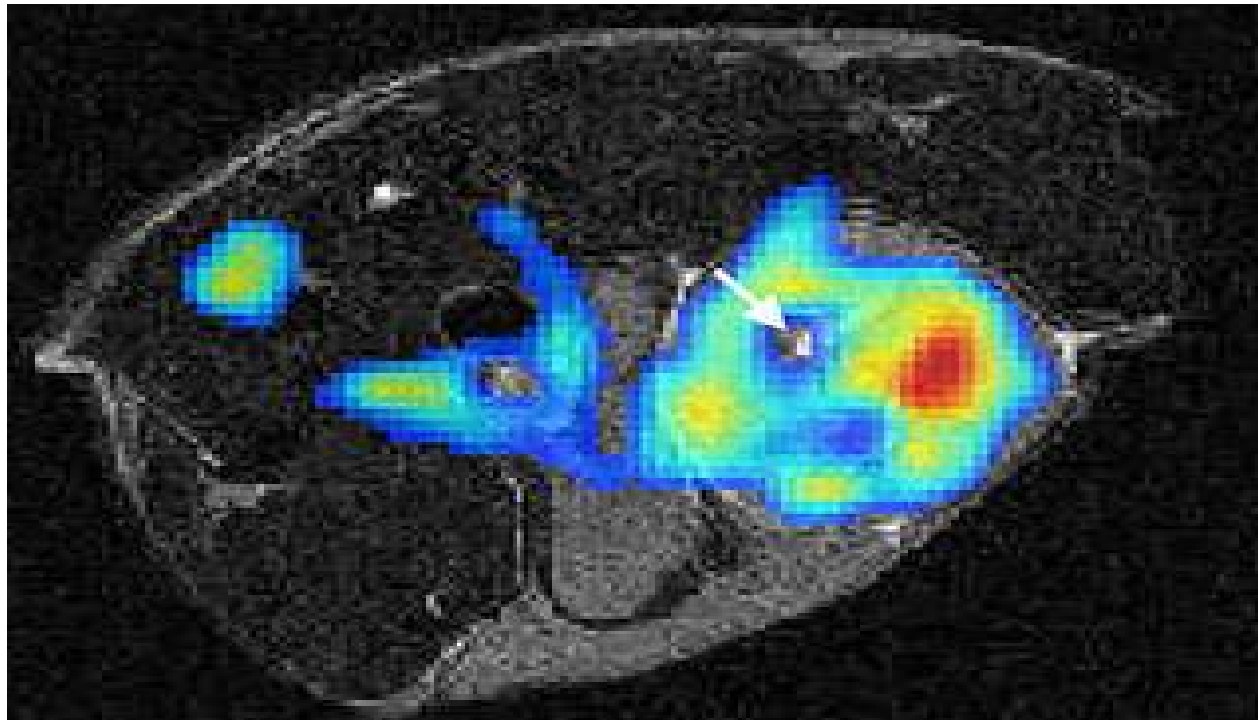


**Figure 20. Combined PET/MRI scan** : the colored area is the PET scan image of a tumor in a lab mouse. The arrow points to a ‘hole’--probably necrotic tissue, in the central part of the tumor. (Source: <http://medicineworld.org/cancer/lead/3-2008/mri-pet-scanner-combo.html> )

# Inter-relations between Nuclear Medicine and Medical Research

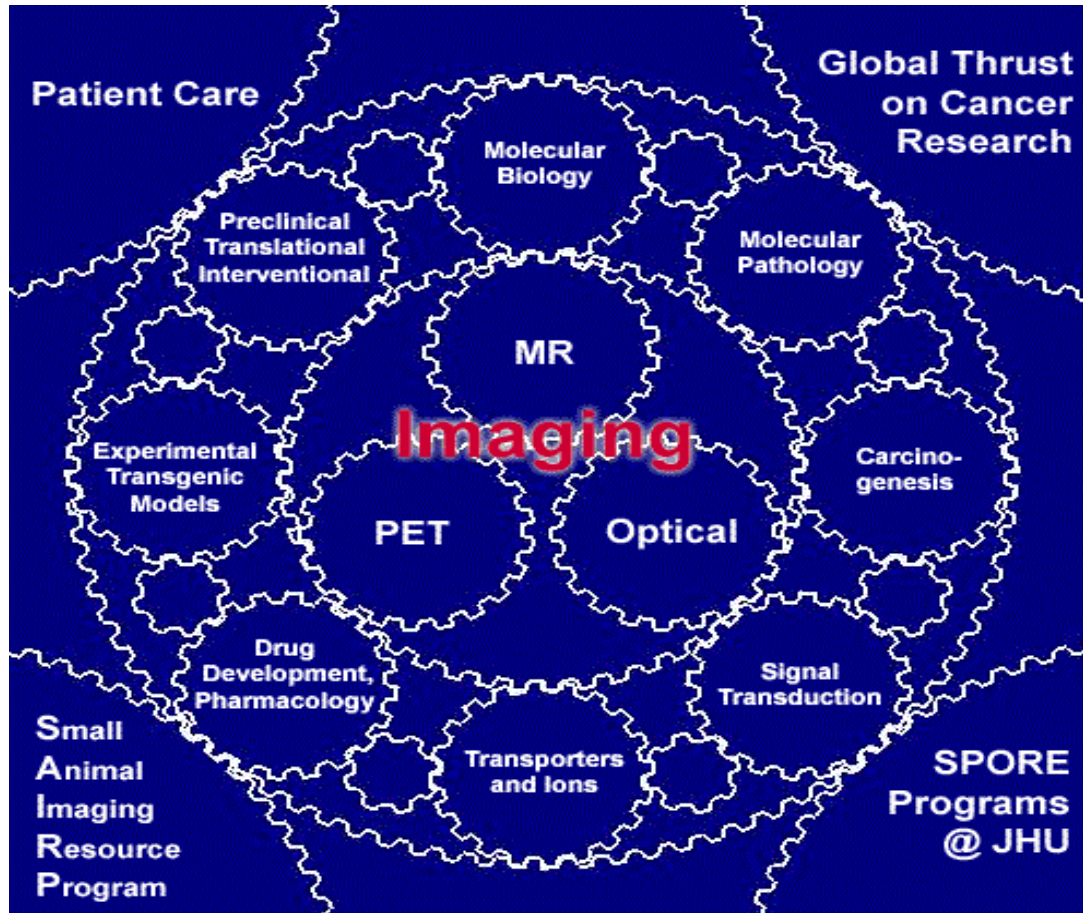


**Figure 21. Nuclear Medicine Imaging and Biomedical Research at JHU.**

Source: In Vivo Cellular Molecular Imaging Center (ICMIC) at John Hopkins University ,

<http://icmic.rad.jhmi.edu/>

# A Markov Chain Mathematical Model of AD

[A. S. Macdonald and D. J. Pritchard. 2000. **A Mathematical Model of Alzheimer's Disease and the ApoE Gene.** *ASTIN Bulletin*, **30**: 69–119 ]

“The great range of genetic diseases arises from the range of effects of the protein products of different alleles, and the (not so) simple combinatorics of inheritance:”

- (1) If an allele encodes a harmless but non-functional protein product, the disease will appear only in homozygous individuals (*autosomal recessive inheritance*, such as in cystic fibrosis).
- (2) Heterozygous cells will produce a mixture of variants of the protein product; if just one of these is **lethal** it will cause disease (*autosomal dominant inheritance*, such as **Huntington's** disease).
- (3) In between these extremes, alleles encode protein products that are more or less dangerous or fully-functional, the effect often depending on the environment. Then different levels of susceptibility to disease will appear, and **homozygous** individuals will often be more susceptible than **heterozygous** individuals.”

# A Mathematical Model of Alzheimer's Disease (A. S. Macdonald and D. J. Pritchard. 2000.)

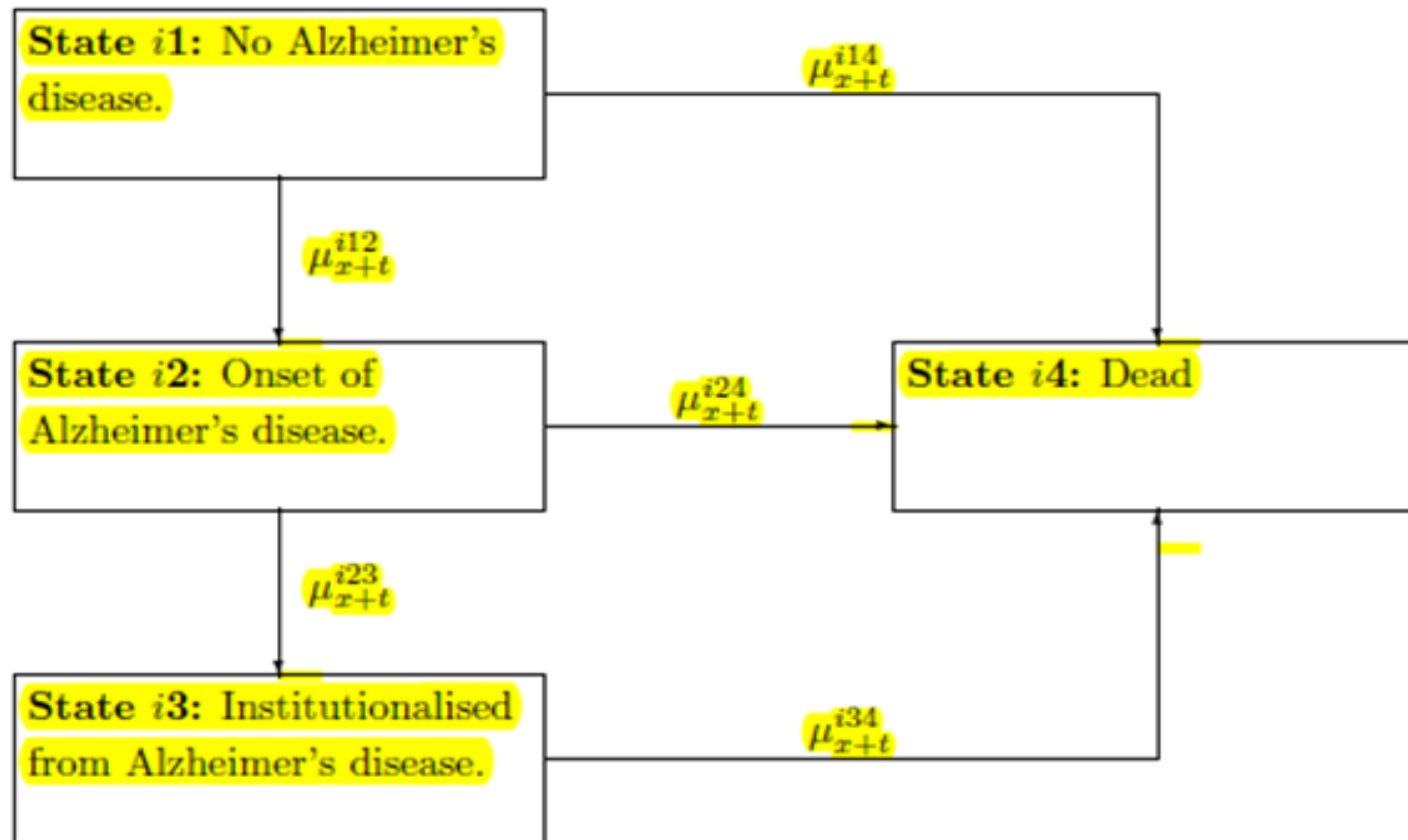


Figure 22. A Simplified Model of Alzheimer's Disease with M subgroups and 4 states.

# AD Model

For use in our model, these odds ratios have to be converted into relative risks. More precisely, we have to find a plausible set of age- and genotype-dependent transition intensities that are consistent with the odds ratios and together are consistent with the aggregate incidence of AD. There is no unique solution to this problem. The method we used was to model the incidence of AD for the  $i$ th genotype as:

$$\mu_{x+t}^{i12} = r_1 f_{x+t}^i \mu_{x+t}^{AD} \quad (12)$$

where:

- (a)  $\mu_{x+t}^{AD}$  is the aggregate incidence rate of AD (from Section 4.3);
- (b)  $f_{x+t}^i$  is a parametric function representing the risk relative to the aggregate incidence rate, where we take  $f_{x+t}^i = 1$  in the case of the  $\varepsilon 3/\varepsilon 3$  genotype; and
- (c)  $r_1$  is a constant chosen so that the aggregate incidence of AD based on the modelled intensities is consistent with the aggregate incidence  $\mu_{x+t}^{AD}$ .

We did this for for males and females separately and combined. We confined our attention to ages 60 and over, in order to get a better fit in the age range of interest in applications. The form of the ORs, either rising to a peak and then falling, or gently declining, suggested a similar pattern of relative risks, and we found the following family of functions satisfactory (note that constant relative risks, or proportional hazards, result in odds ratios with exponential growth):

$$f_{x+t}^i = E e^{-F((x+t)-k_1)^2 - G((x+t)-k_2)} + H. \quad (13)$$



## AD Model Results-1 (*loc.cit.*)

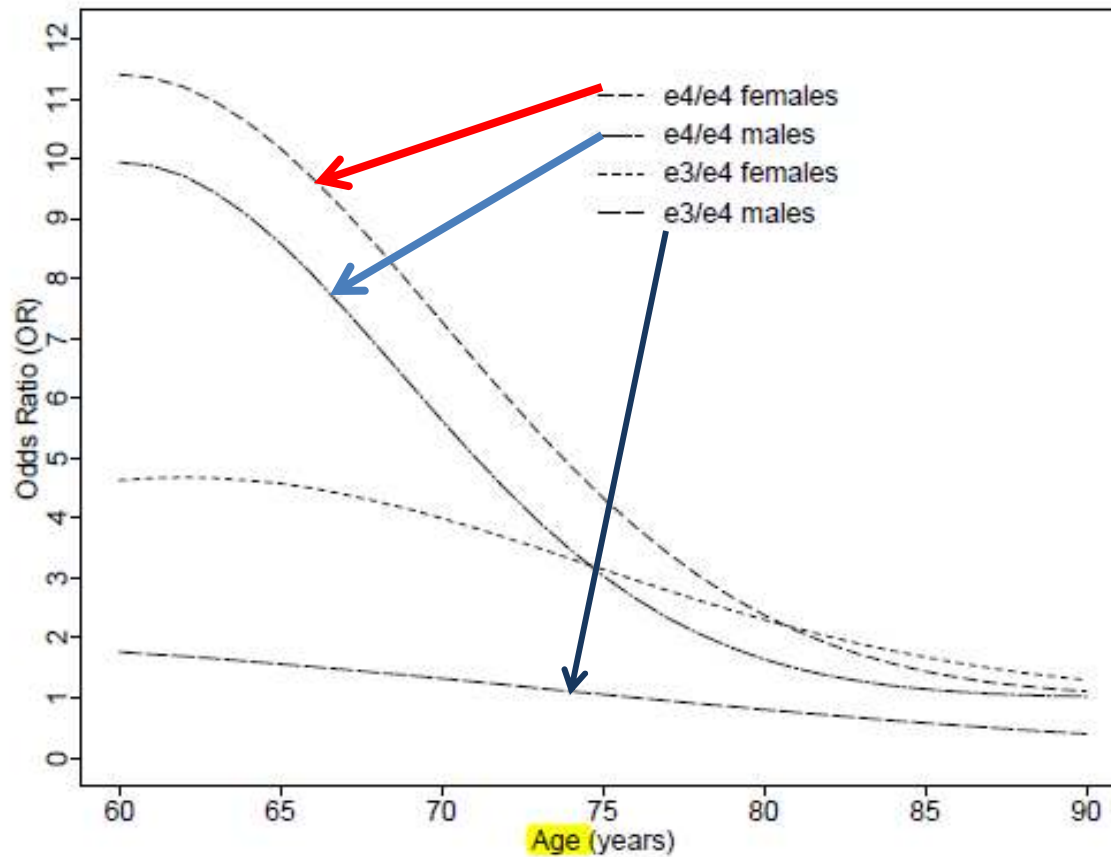


Figure 8: Modelled risk of AD, relative to the  $\epsilon_3/\epsilon_3$  genotype, for  $\epsilon_4/\epsilon_4$  and  $\epsilon_3/\epsilon_4$  genotypes. Based on odds ratios from Farrer *et al.* (1997).

# AD Model Results-2 (*loc.cit.*)

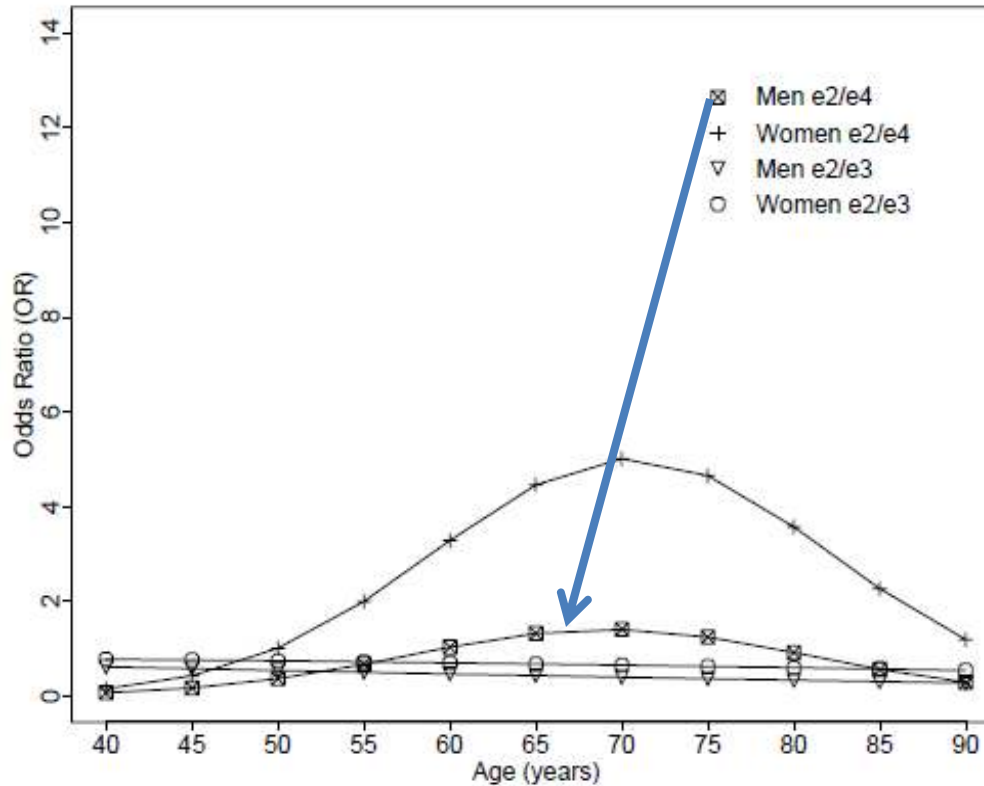


Figure 6: Odds ratios (ORs) of AD relative to  $\epsilon_3/\epsilon_3$  genotype for  $\epsilon_2/\epsilon_2$  or  $\epsilon_2/\epsilon_3$  and  $\epsilon_2/\epsilon_4$  genotypes. Source: Farrer *et al.* (1997).

# AD Model for Survival Times of AD Patients (loc.cit.)

Table 2: Summary Statistics on Survival Times of AD Patients.

Reference	Mean (Median) Age at Onset	Mean (Median) Survival Time	Addition to $\mu_{x+t}^{34}$
Barclay <i>et al.</i> (1985a)	(73.3) yrs	(8.1) yrs	0.15829
Bracco <i>et al.</i> (1994)	(72.4) yrs	7.3 yrs	0.25259
Diesfeldt <i>et al.</i> (1986)	75.6 yrs	7.2 yrs	0.21056
Heyman <i>et al.</i> (1996)	(69.2) yrs	(9.7) yrs	0.10993
Jost <i>et al.</i> (1995)	75.1 yrs	8.11 yrs	0.13345
Kokmen <i>et al.</i> (1988)	80.4 yrs	6.2 yrs	0.26420
Treves <i>et al.</i> (1986)	73.9 yrs	(9.3) yrs	0.08135
Average			0.17291

$$E \left[ x + \int_x^\omega I_1(t) dt \mid N_{12}(\omega - x) = 1 \text{ and } I_1(x) = 1 \right] = x + \frac{\int_x^\omega (t - x) \mu_t^{12} P_{xt}^{11} dt}{\int_x^\omega \mu_t^{12} P_{xt}^{11} dt} \quad (9)$$

# Is AD a Multifactorial Disorder ?

- ``(i). Lifestyle and environment can affect the potency of susceptibility genes. For example, the activity of the protein produced by a *dangerous* allele may be enhanced in certain environments, or a *protective* allele may be put at greater risk of being knocked out by a mutation.
- (ii). Although the outline in the previous slide mentioned only single genes, most processes in the human body are complicated (**highly complex ?!**) and involve very many proteins, each encoded by its own gene with its various alleles. **Most genetic disease will result from combinations of several alleles, lifestyle and environment;** the term for this is **multifactorial disorder** “ (*loc. cit*).
- ***In the case of AD there are only six genotypes linked to ApoE*** (which is involved in lipoprotein metabolism):  $\epsilon 2/\epsilon 2$ ,  $\epsilon 2/\epsilon 3$ ,  $\epsilon 2/\epsilon 4$ ,  $\epsilon 3/\epsilon 3$ ,  $\epsilon 3/\epsilon 4$ , and  $\epsilon 4/\epsilon 4$ ;  
this is unlike cancer cases where there are **many thousands of genotypes** involved, so there can be *many* types of multifactorial disorders!

# AD Model Parameters (*loc.cit.*)

Table 7: Parameters for the Relative Risk of AD for Males, Females and in Aggregate, by Genotype.

Gender	Genotype	Parameter Values						
		E	F	G	H	$k_1$	$k_2$	$r_1$
Both	$\epsilon_4/\epsilon_4$	13.5	0.00529	0	1	60	–	0.93
	$\epsilon_3/\epsilon_4$	2.98	0.00312	0	1	62	–	
	$\epsilon_2/\epsilon_4$	2.87	0.00938	0	1	68	–	
	$\epsilon_2/\epsilon_2$ & $\epsilon_2/\epsilon_3$	0.754	0	0.00859	0	–	60	
Female	$\epsilon_4/\epsilon_4$	10.4	0.00504	0	1	60	–	0.88
	$\epsilon_3/\epsilon_4$	3.68	0.00319	0	1	62	–	
	$\epsilon_2/\epsilon_4$	4.21	0.0102	0	1	68	–	
	$\epsilon_2/\epsilon_2$ & $\epsilon_2/\epsilon_3$	0.675	0	0.00692	0	–	60	
Male	$\epsilon_4/\epsilon_4$	8.94	0.00656	0	1	60	–	1.27
	$\epsilon_3/\epsilon_4$	1.92	0.00103	0	0	51	–	
	$\epsilon_2/\epsilon_4$	1.42	0.00506	0	0	67	–	
	$\epsilon_2/\epsilon_2$ & $\epsilon_2/\epsilon_3$	0.434	0	0.0160	0	–	60	

## New Strategies:

- II. Making and using antibodies for modified  $A\beta$  and  $\tau$ -proteins, combined with
- III. Novel Molecular Imaging;
- IV. Improved AD Supercomputer Modeling, maybe combined with
- V. **Radioimmunotherapy (RIT) and Gene Therapy.**

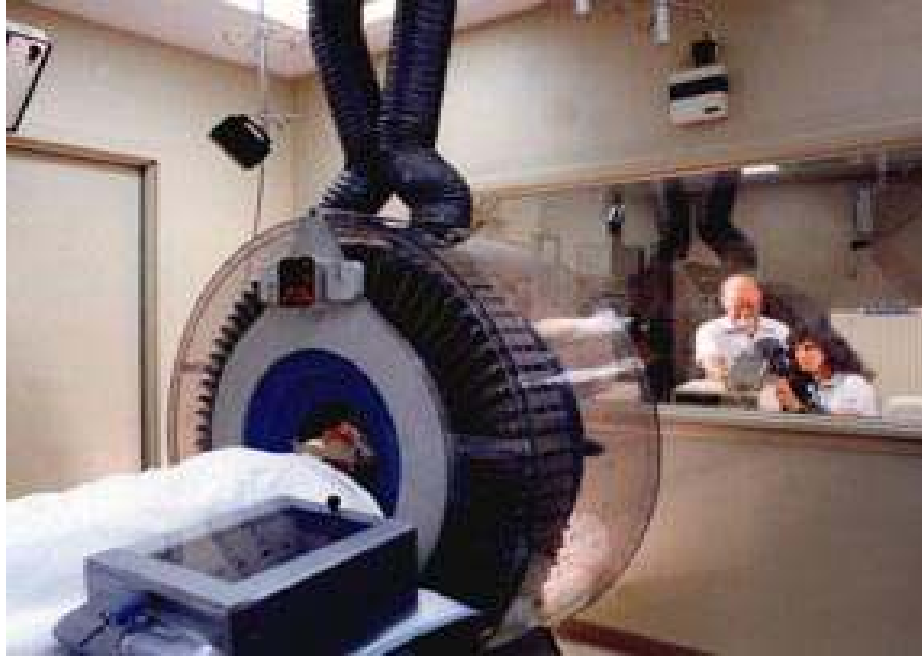
### **Major Obstacles:**

1. Failed AD Clinical trials in UK with an attempted 'vaccination'.
2. The high cost of screening large number of patients by PET/CAT and/or NMRI.

### **Possible answers in the near future:**

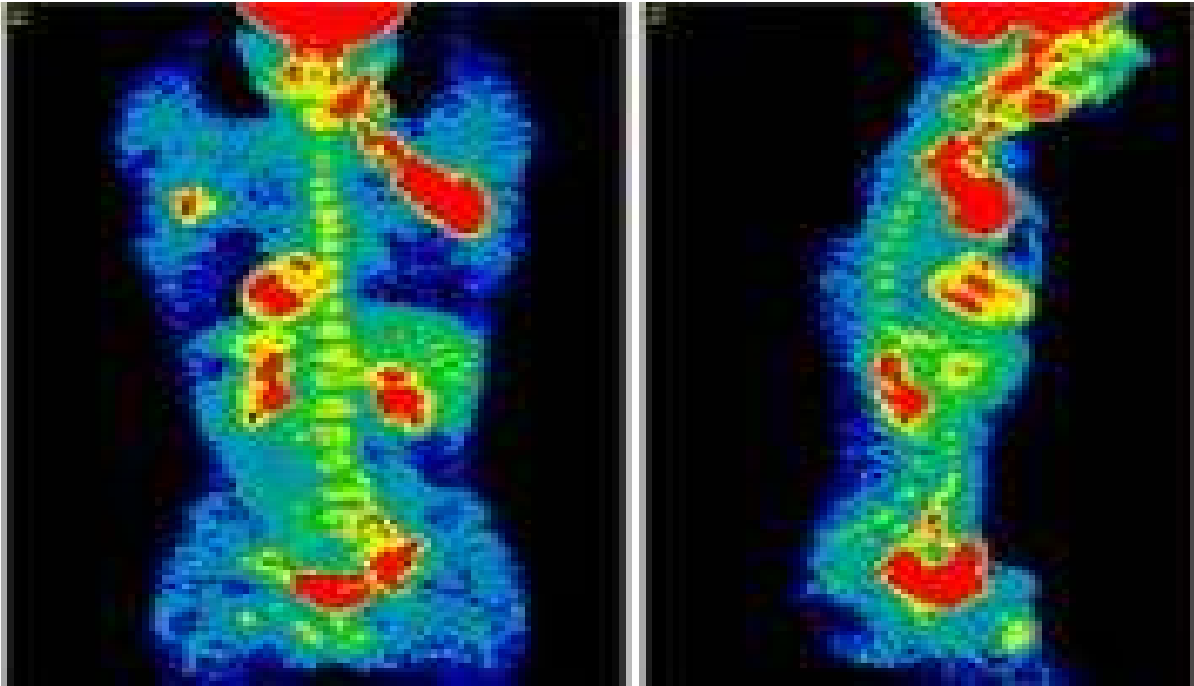
- Improved Modeling may help, for example, with designing new clinical trials and animal studies that are now needed. This is a low-cost exercise involving minds, supercomputers, data mining and mega-database analyses.
- **Novel molecular imaging** techniques that are less expensive than PET/CT and MRI/PET. An example already employed for early discovery of cancers is Near Infrared Fluorescence Spectroscopy (NIRFS).
- **RIT** or **Radioimmunotherapy** where the goal is to target with radioisotopes or markers the affected cells or aggregated molecules without harming the healthy cells. This is also known as **cell-directed therapy**. In cancers, RIT success was achieved with the radioisotopes irridium-192 and iodine-125 to treat lymphomas and thyroid tumors, respectively.

## Figure 23. PET Imaging of Tumors with FDG at BNL



**Cancer tumors over-utilize glucose, and the PET scan identifies the metabolic difference between normal tissue and the tumor FDG labeling, thus identifying tumors.**

## Fig.24. PET with FDG can predict response to Chemotherapy



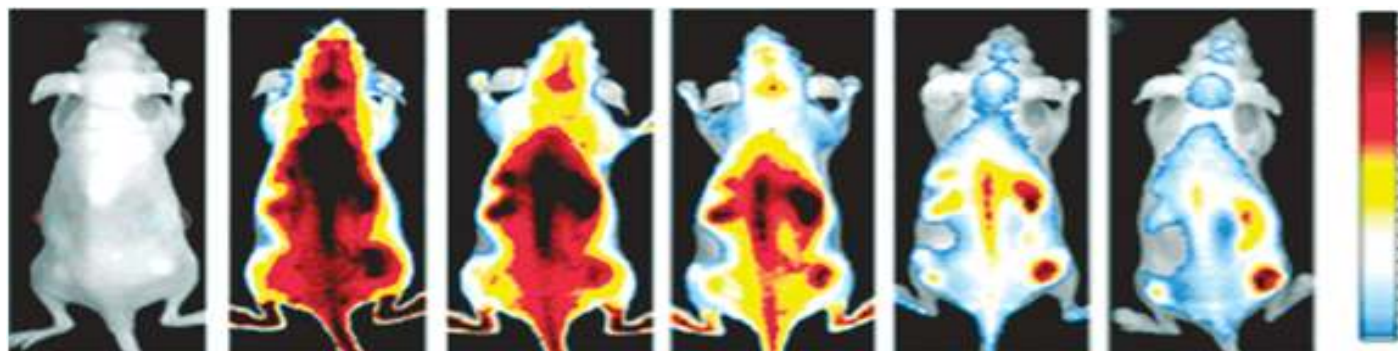
“Our study demonstrates that patients who respond to chemotherapy can be identified early in the course of their therapy, and these patients will generally exhibit prolonged overall survival,” (Claude Nahmias, Professor of Radiology and Medicine at the University of Tennessee Medical Center in Knoxville, a co-author of the report ***“Time Course of Early Response to Chemotherapy in Non-Small Cell Lung Cancer Patients With 18F-FDG PET/CT”***, *Journal of Nuclear Medicine*, 2011 ). **However, the F-18 FDG PET scan images shown above are not for Early Cancers!**



# Early Diagnosis of Cancer: Near Infrared Fluorescence NIRF Imaging at the Molecular Level

- Near Infrared Fluorescence NIRF Imaging <sup>1,2</sup>:

- Pre-scan      5 min      30 min      2 hr      6 hr      24 hr



- **FIGURE 25** . Real time *in vivo* NIR fluorescence images of KB/HT1080 **dual tumor mice** with I.V. injection of DiR-LDL-FA (**5.8  $\mu$ M**)<sup>\*2</sup>. (Reproduced with permission from Ref 60. Copyright 2007 American Chemical Society). **1,1-dioctadecyl-3,3,3, 3-tetramethylin-dotricarbocyanine iodide** (DiR)-based NIR fluorescent label.
- **1.** Baianu, I. C. et al. 2004. NIR and Fluorescence Microspectroscopy, IR Chemical Imaging and H-R NMR Analysis of Intact Soybean Seeds, Embryos and **Single Cancer Cells**, Ch. 12 in: *Analysis of Oil Seeds, AOCs Publs*, pp. 243-278.

**2.** [Wiley Interdisciplinary Reviews: Nanomedicine and Nanobiotechnology, Volume 2, Issue 4](#), Xiaoxiao He, Kemin Wang and Zhen Cheng. Article first published online: **26 March 2010**.

**3.** <http://www.youtube.com/watch?v=VEnCww0JmYU> (Stanford University Seminar).

# NIR Fluorescence Molecular Imaging Probe

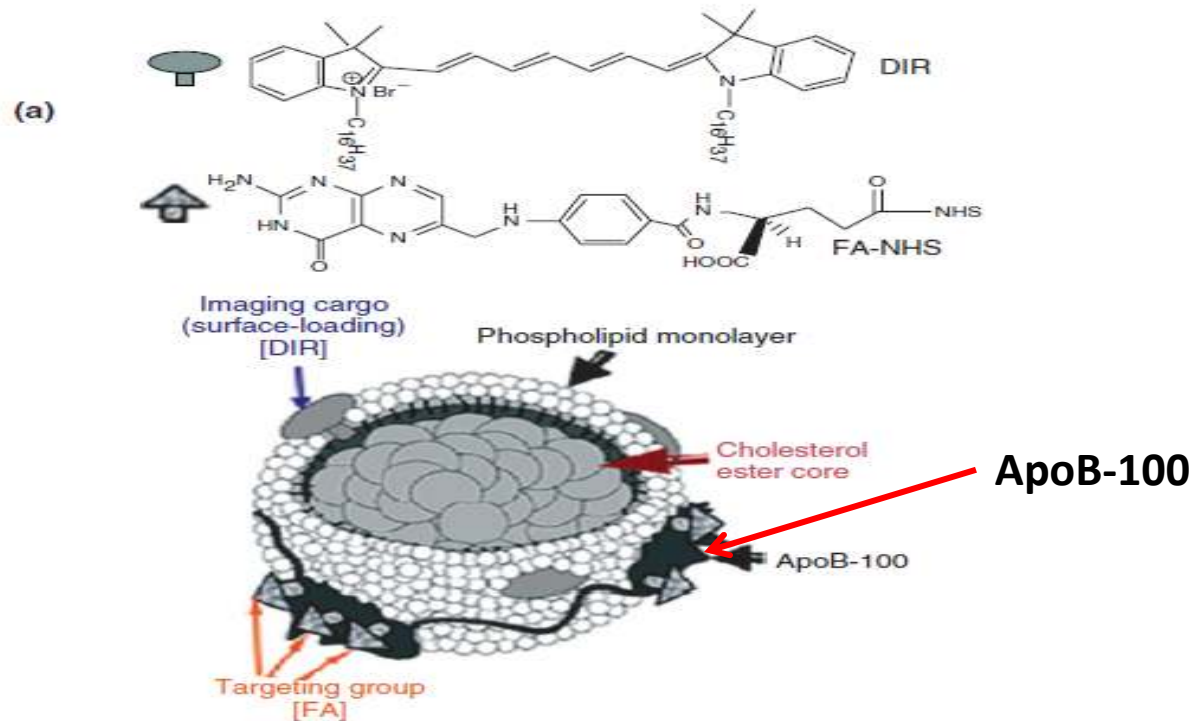


**Figure 26.** Source: Ref. 2. [Wiley Interdisciplinary Reviews: Nanomedicine and Nanobiotechnology, Volume 2, Issue 4](#), Xiaoxiao He, Kemin Wang and Zhen Cheng. Article first published online: **26 March 2010.**

**3--5.** Gratton, G. et al. 1998. **Memory-driven Processing in the Human Medial Occipital Cortex: an Event Related Optical Signal (EROS) study**, *Psychophysiology*, **38: 348-351**; *Optical Engineering (1995)* **34:32-42**; *Phys. Med. Biol.*, **4**: 308-314.

# NIRFS Enhanced via Nanoprobes

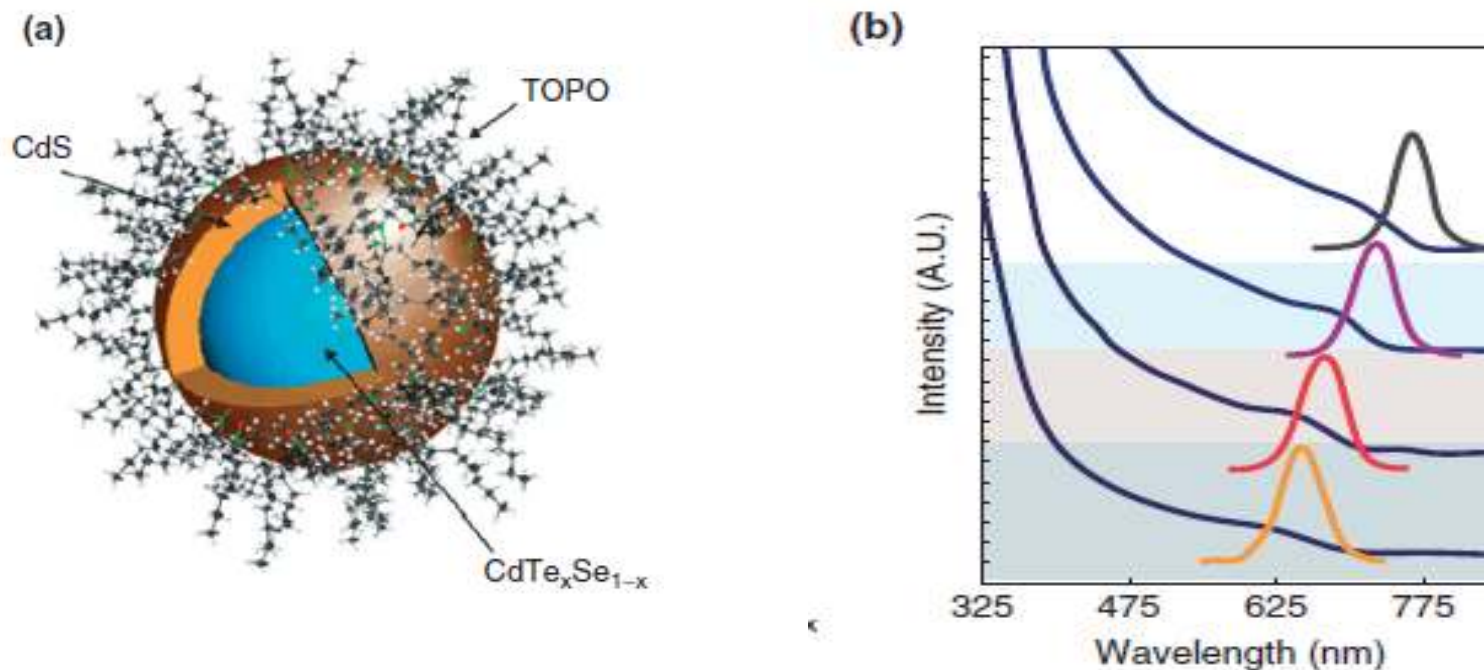


**FIGURE 27.** “Schematic and optical properties of CdS-capped CdTe<sub>x</sub>Se<sub>1-x</sub> alloyed near-IR-emitting quantum dots (QDs). (a) Biocompatible near-IR-emitting QDs contain a core structure (CdTe<sub>x</sub>Se<sub>1-x</sub>) with a CdS and an organic shell. (Reproduced with permission from Ref 74. Copyright 2006 American Chemical Society). (b) Absorbance and fluorescence spectra of CdS-capped CdTe<sub>x</sub>Se<sub>1-x</sub> near-IR-emitting QD with different compositions of Te:Se in the core (*loc.cit*)”<sup>2</sup>.

**100-Fold Sensitivity Enhancement**  **Single Molecule Detection Capabilities.**

# NIRFS Detection of Tumors with NIR-emissive Polymersomes in Rats

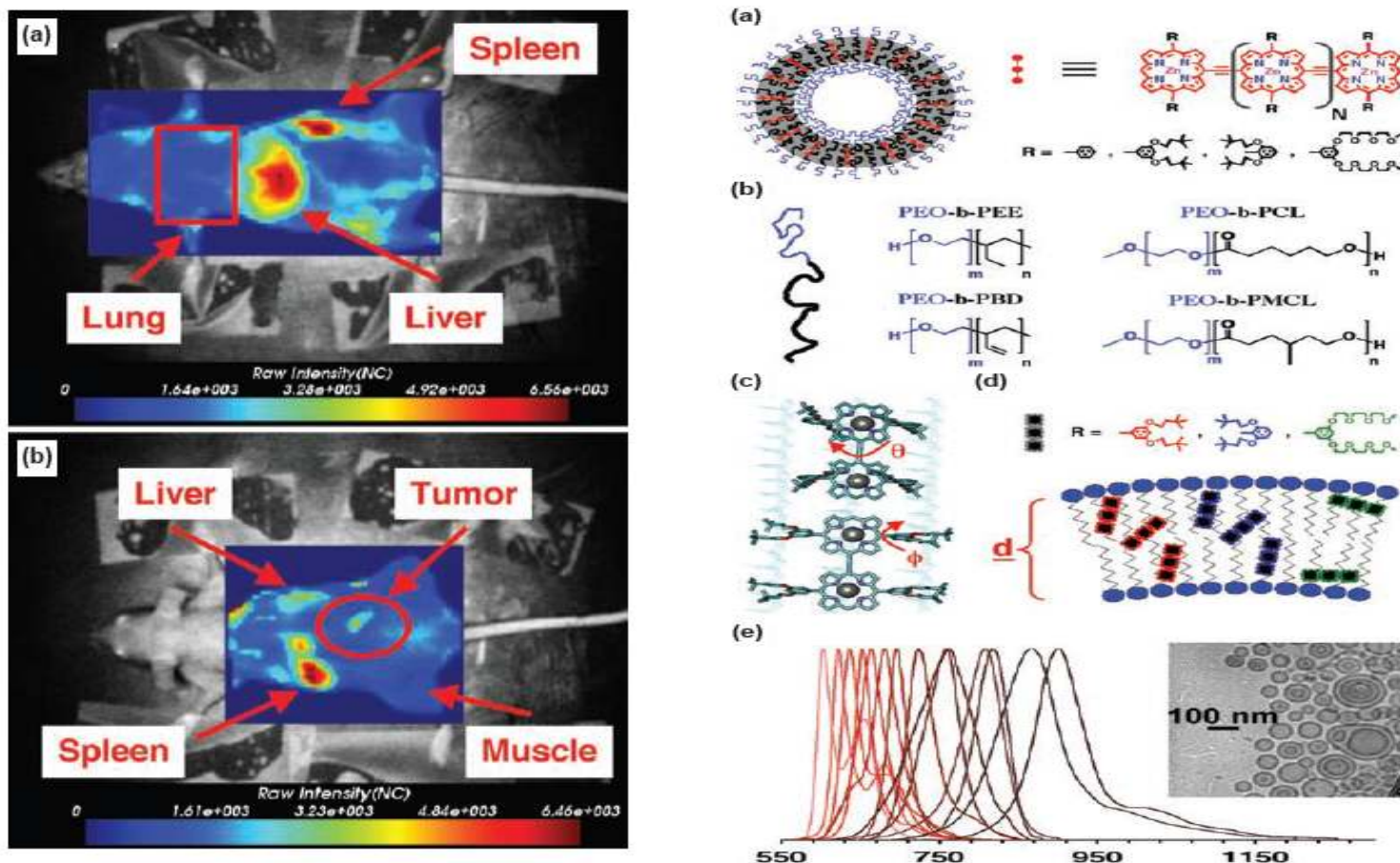


**Figure 2b.** Source: GHORUGHCHIAN, P. et al. 2009. *in vivo* fluorescence imaging: a personal perspective, [NANOMEDICINE AND NANOTECHNOLOGY, VOL 1, ISSUE 2 \(MARCH/APRIL 2009\)](#), 156-167. DOI: 10.1002/wnan.7 <http://wires.wiley.com/WileyCDA/WileyArticle/wisid-WNAN7.html> : **Left a. & b: NIRFS detection of rat tumors.**

150-nm diameter nondegradable polymersomes (composed of a 1 : 1 molar mixture of PEO30-b-PBD46 and PEO80-b-PBD125; 1 : 40 NIRF-to-total-polymer molar ratio) were imaged after tail-vein injection of tumor-bearing mice utilizing a GE eXplore Optix instrument ( $\lambda_{ex} = 785 \text{ nm}$ ,  $\lambda_{em} = 830\text{--}900 \text{ nm}$ ).

# CONCLUSIONS

- Early discovery of Alzheimer's Disease is the key to finding treatments for AD and to prevent the worsening of AD patients' condition
- This is a problem of great importance and urgency for humanitarian, social and also economical reasons, with \$ trillion consequences over the next decades if not solved soon; recent advances in nuclear medicine imaging—diagnosis of AD through PET scanning— give hope for early discovery of AD.
- Novel approaches are needed to early discovery and treatments of AD; these may involve combinations of nuclear medicine imaging with advanced supercomputer modeling and other molecular imaging and biochemical diagnostic techniques capable of both high specificity and high sensitivity; low cost alternatives are needed to allow noninvasive screening of large subpopulations that may be at risk for AD.

# REFERENCES

- **“Early diagnosis of Alzheimer's disease” edited by Leonard F. M. Scinto and Kirk R. Daffner (2010), pp. 875.**
- Ashburner, M, et al.2000. Gene Ontology: A Tool for the Unification of Biology. The Gene Ontology Consortium, *Nature Genetics*, **25(1): 2529.**
- **Baianu, I.C., Editor. “Nuclear Medicine, Diagnostic Tomography and Imaging: Early Medical Diagnosis using Nuclear Medicine Techniques” , Minuteman Press, USA, pp. 554, Second Edition.**
- Baianu, IC, Editor. 2011. *Complex Systems Biology*. Minuteman Press: USA, pp. 545. *Ibid.*2010. *Symbolic Dynamics and Dynamical System Models, Volumes I to III, Minuteman Press, pp. 1,046.*
- Baianu, IC. 2007. **Categorical Ontology of Levels and Emergent Complexity: An Introduction, *Axiomathes*, 17 (3-4): 209-222**
- Baianu, IC. 2006. Robert Rosen’s Work and Complex Systems Biology, *Axiomathes*, **16 (1-2): 25-34.**
- Baianu, IC.1986. Computer Models and Automata Theory in Biology and Medicine, *Mathematical Modelling*, **7: 1513-1557. In: *Mathematical Models in Medicine, M. Witten, Editor, Pergamon Press: New York. 10***
- Baianu, IC. 1977. *A Logical Model of Genetic Activities in Lukasiewicz Algebras: The Nonlinear Theory. *Bulletin of Mathematical Biology*, 39: 249-258.*
- Baianu, IC, Glazebrook, JF, and Brown R. 2011. A Category Theory and Higher Dimensional Algebra Approach to Complex Systems Biology, Meta-systems and Ontological Theory of Levels. *Conference Proceedings: Understanding Intelligent and Complex Systems. B. Iantovics et al, eds. (accepted, in press)*
- Baianu, IC and Poli, R. 2011. From Simple to Super- and Ultra- Complex Systems: A Paradigm Shift Towards Non-Abelian Emergent System Dynamics, *loc.cit.*
- Baianu, IC. and Glazebrook, JF. 2010. Categorical Ontology of Complex Systems, Meta-Systems and Levels, *BRAIN - Special Issue on Complexity in Sciences and Artificial Intelligence, B. Iantovics, et al, editors, 1: 118-207*
- Baianu, IC. et al. 2010. **Lukasiewicz-Moisil Many-Valued Logic Algebras of Highly-Complex Systems, *BRAIN. loc.cit, pp. 1- 12***
- Baianu, IC, Brown, R and Glazebrook, JF.2007. Categorical Ontology of Complex Spacetime Structures: The Emergence of Life and Human Consciousness. *Axiomathes*, **17: 223–352.**
- Baianu, IC, et al. 2006. Complex Nonlinear Biodynamics: Transformations of Neuronal, Genetic and Neoplastic Networks, *Axiomathes. 16 (1-2): 65—122*
- Baianu, IC and Prisecaru, V. 2005. Complex Systems Analysis of Cell Cycling Models in Carcinogenesis, preprint *arXiv/q-bio.OT/0406045: pp.23*
- Baianu, IC et al. 2004. NIR and Fluorescence Microspectroscopy, IR Chemical Imaging and H-R NMR Analysis of Intact Soybean Seeds, Embryos and Single Cells, Ch. 12 in: *Analysis of Oil Seeds, AOCS Publs, pp. 243-278.*
- Bard, J, Rhee, SY, and Ashburner, M. 2005. An ontology for cell types, *Genome Biol*, **6(2), R21**
- Bogaard, A et al. 2009. Interaction of Cellular and Network Mechanisms in Spatiotemporal Pattern Formation in Neuronal Networks, *The Journal of Neuroscience*, **29(6):1677–1687**

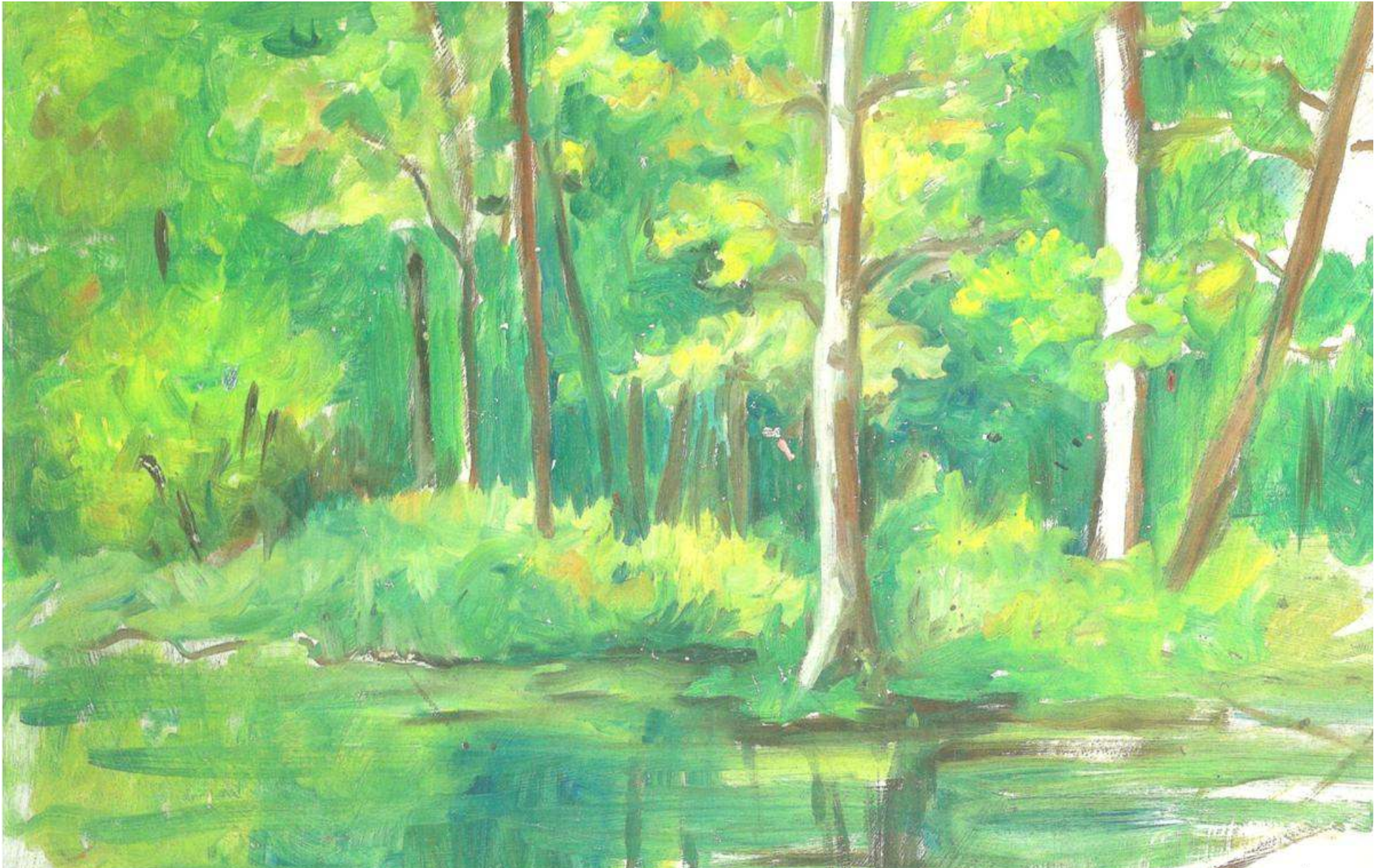
- Brown, R, Paton, R and Porter, T. 2004. Categorical language and hierarchical models for cell systems, in *Computation in Cells and Tissues*, Paton, R. et al (Eds.), Springer Verlag, pp. 289-303.
- Casti, JL and Karlqvist, A. 1986. *Complexity, Language, and Life: Mathematical Approaches*. Springer-Verlag: Berlin, etc. pp.298. (International Institute for Applied Systems Analysis).
- Charles, M., Baianu, I.C. and Prisecaru, V. 2007. Visual Molecular Dynamics (VMD), the Impact of Lectins on Alzheimer's Disease Treatment and Its Side Effects, RAP/YSP Program, YSP Excellent Presentation Award.
- Craft, DL, Weins, LM, Selkoe, DJ. 2002. A Mathematical Model of the Impact of Novel Treatments on the A $\beta$  Burden in the Alzheimer's Brain, CSF and Plasma, *Bulletin of Mathematical Biology*, **64**: 1–21.
- Fleischaker, G. 1988. Autopoiesis: the Status of its System Logic, *Biosystems*, **22(1)**: 3749.
- Gnoli, C and Poli, R. 2004. Levels of Reality and Levels of Representation, *Knowledge Organization*, **21(3)**: 151-160.
- Gratton, G et al. 1998. Memory-driven Processing in the Human Medial Occipital Cortex: an Event Related Optical Signal (EROS) study, *Psychophysiology*, **38**: 348-351; *Optical Engineering (1995)* **34**:32-42; *Phys. Med. Biol.*, **4**: 308-314 11
- Golubitsky, M, and Stewart, I. 2006. Nonlinear Dynamics and Networks: the groupoid formalism, *Bulletin of the AMS*, **43**:305-364
- Keogh, E K, Mehrotra, S and Pazzani, M.2002. Locally Adaptive Dimensionality Reduction for Indexing Large Time Series Databases, *ACM Transactions on Database Systems*, **27(2)**: 188-228
- Macdonald, A S and Pritchard, D J. 2000. A Mathematical Model of Alzheimer's Disease and the ApoE Gene. *ASTIN Bulletin*, **30**: 69–119
- Mani, S et al. 1997. Dementia Screening with Machine Learning Methods, *AMIA Annual Fall Symposium, Nashville*; *Differential Diagnosis of Dementia: A Knowledge Discovery and Data Mining (KDD) Approach*, loc.cit.
- Maturana, H., and Varela, F. J. (1980). *Autopoiesis and Cognition: The Realization of the Living*. D. Reidel: Boston

# References

- Massoud, T.F. and Gambhir, S.S. 2003. Molecular Imaging in Living Subjects: Seeing Fundamental Biological Processes in a New light, **17 (5): 545-580**
- Nakao, H and Mikhailov, A S.2010. Turing Patterns in Network-organized Activator-inhibitor Systems, *Nature Physics*, **6: 544-550**
- [Naito A](#), [Kawamura I](#). **Solid-state NMR as a method to reveal structure and membrane-interaction of amyloidogenic proteins and peptides.** *Biochim Biophys Acta*. 2007 Aug 17,**68(8):1900-12**. Epub 2007 Apr 5.
- Poli, R. 2006. Levels of Reality and the Psychological Stratum, *Revue internationale de philosophie*, **61 (2): 163-180**.
- Poli, R. 2006. The Theory of Levels of Reality and the Difference Between Simple and Tangled Hierarchies. In: *Systemics of Emergence. Research and Development*, Minati , G., Pessa, E., Abram M. eds. Berlin: Springer, pp.715-722.
- Poli, R. 2002. Ontological Methodology, *International Journal of Human-Computer studies*, **56: 639-664**.
- Puri, IK and Li, L.2010. Mathematical Modeling for the Pathogenesis of Alzheimer's Disease, *PLoS ONE*, **5(12): e15176**
- Shankle, WR et al. 1997. Detecting Very Early Stages of Dementia from Normal Aging with Machine Learning methods, In Keravnou, E, et al, editors, *Artificial Intelligence in Medicine, AIME97*, volume **1211: 73-85**, Springer: Berlin.
- Wallace, R. 2005. *Consciousness: A Mathematical Treatment of the Global Neuronal Workspace Model*, Springer: New York.
- Wallace, R. 2011. The cultural epigenetics of psychopathology: The missing heritability of complex diseases found? In: *Transactions on Computational Systems Biology XIII*, Vol. **6575: 131--170**. Editor-in-chief: Priami Corrado.
- Wallace, D and Wallace, R. 2000. Life and death in Upper Manhattan and the Bronx, *Environment and Planning A*, **32:1245-1266**.
- Yamamoto, S et al. 2004. An Ontology for Annotation of Signal Transduction Pathway Molecules in the Scientific Literature: Molecule Role Ontology, *Comparative and Functional Genomics*. **5 (6-7): 528-536**.



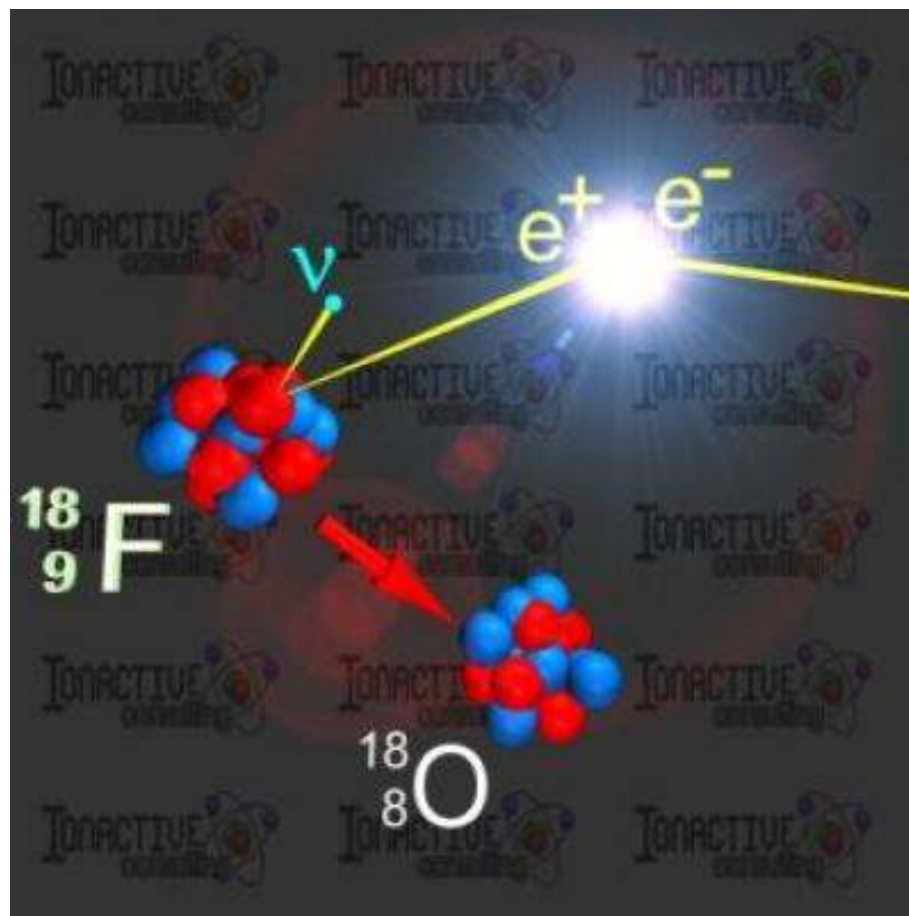
# Questions



Landscape



# Answers



# Structure and morphology of the Alzheimer's amyloid fibril

*Microscopy Res Tech.* 2005 Jul;67(3-4):210-7.

**Structure and morphology of the Alzheimer's amyloid fibril.**

[Stromer T](#), [Serpell LC](#). Department of Biochemistry, School of Life Sciences, University of Sussex, Falmer, BN1 9QG, UK.

## **Abstract**

Amyloid fibrils are deposited in a number of diseases, including Alzheimer's disease, Type 2 diabetes, and the transmissible spongiform encephalopathies (TSE). These insoluble deposits are formed from normally soluble proteins that assemble to form fibrous aggregates that accumulate in the tissues. Electron microscopy has been used as a tool to examine the structure and morphology of these aggregates from ex vivo materials, but predominantly from synthetic amyloid fibrils assembled from proteins or peptides in vitro. Electron microscopy has shown that the fibrils are straight, unbranching, and are of a similar diameter (60-100 Angstroms) irrespective of the precursor protein. Image processing has enhanced electron micrographs to show that amyloid fibrils appear to be composed of *protofilaments wound around one another*. In combination with other techniques, including X-ray fiber diffraction and solid state NMR, electron microscopy has revealed that the internal structure of the amyloid fibril is a *ladder of beta-sheet* structure arranged in a cross-beta conformation.

# Structure and texture of fibrous crystals formed by Alzheimer's Abeta(11-25) and (1-40) peptide fragment/Amyloid Fibrils

*Structure*. 2003 Aug;11(8):915-26.

**Structure and texture of fibrous crystals formed by Alzheimer's abeta(11-25) peptide fragment.** [Sikorski P](#), [Atkins ED](#), [Serpell LC](#). Physics Department, University of Bristol, Tyndall Avenue, Bristol BS8 1TL, United Kingdom.

## Abstract

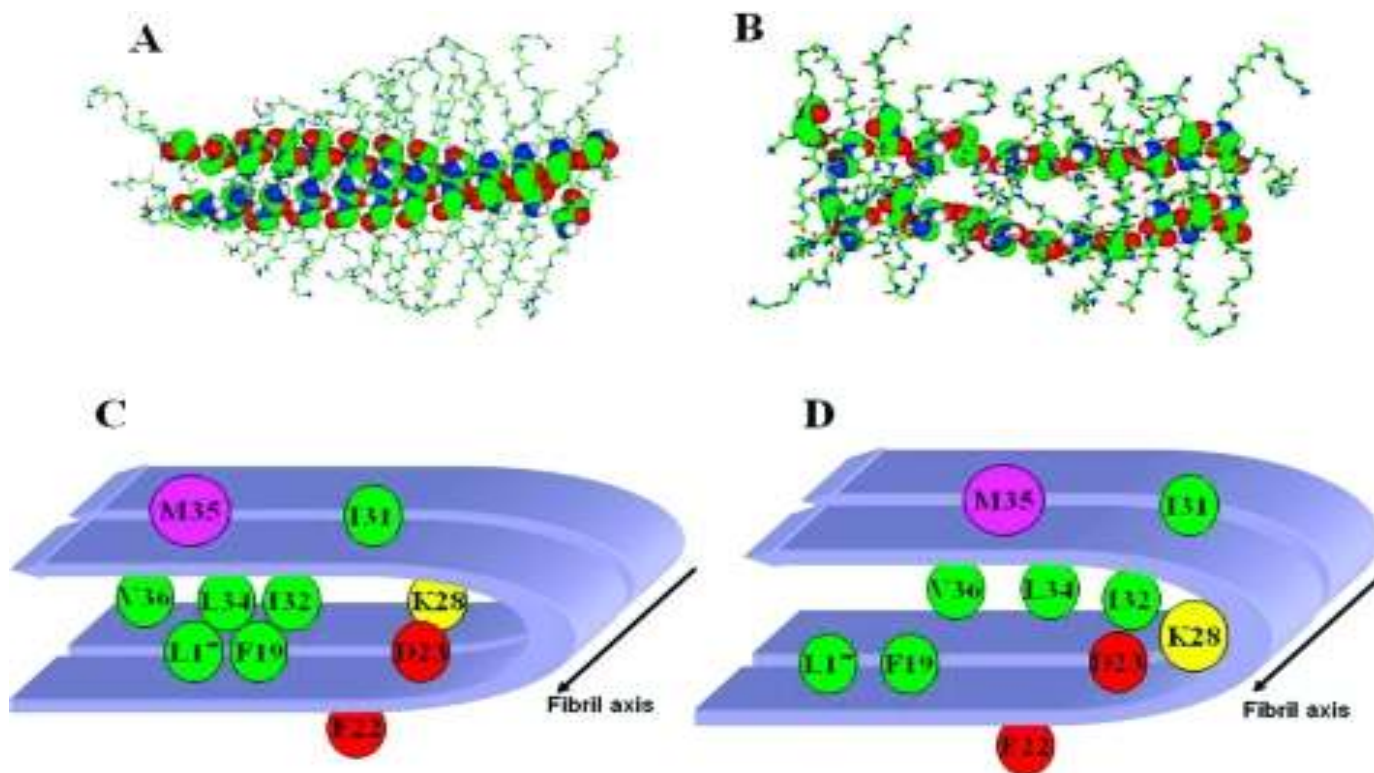
Amyloid fibril deposition is central to the pathology of Alzheimer's disease. X-ray diffraction from amyloid fibrils formed from full-length Abeta(1-40) and from a shorter fragment, Abeta(11-25), have revealed **cross-beta diffraction** fingerprints. Magnetic alignment of Abeta(11-25) amyloid fibrils gave a distinctive X-ray diffraction texture, allowing interpretation of the diffraction data and a model of the arrangement of the peptides within the amyloid fiber specimen to be constructed. An intriguing feature of the structure of fibrillar Abeta(11-25) is that the **beta sheets, of width 5.2 nm**, stack by slipping relative to each other by the length of two amino acid units (0.70 nm) to form **beta ribbons 4.42 nm** in thickness. **Abeta(1-40)** amyloid fibrils likely consist of **once-folded hairpins**, consistent with the size of the fibers obtained using electron microscopy and X-ray diffraction.

# Alzheimer Abeta amyloid aggregates

*Chem Rev.* 2010 Aug 11;110(8):4820-38.

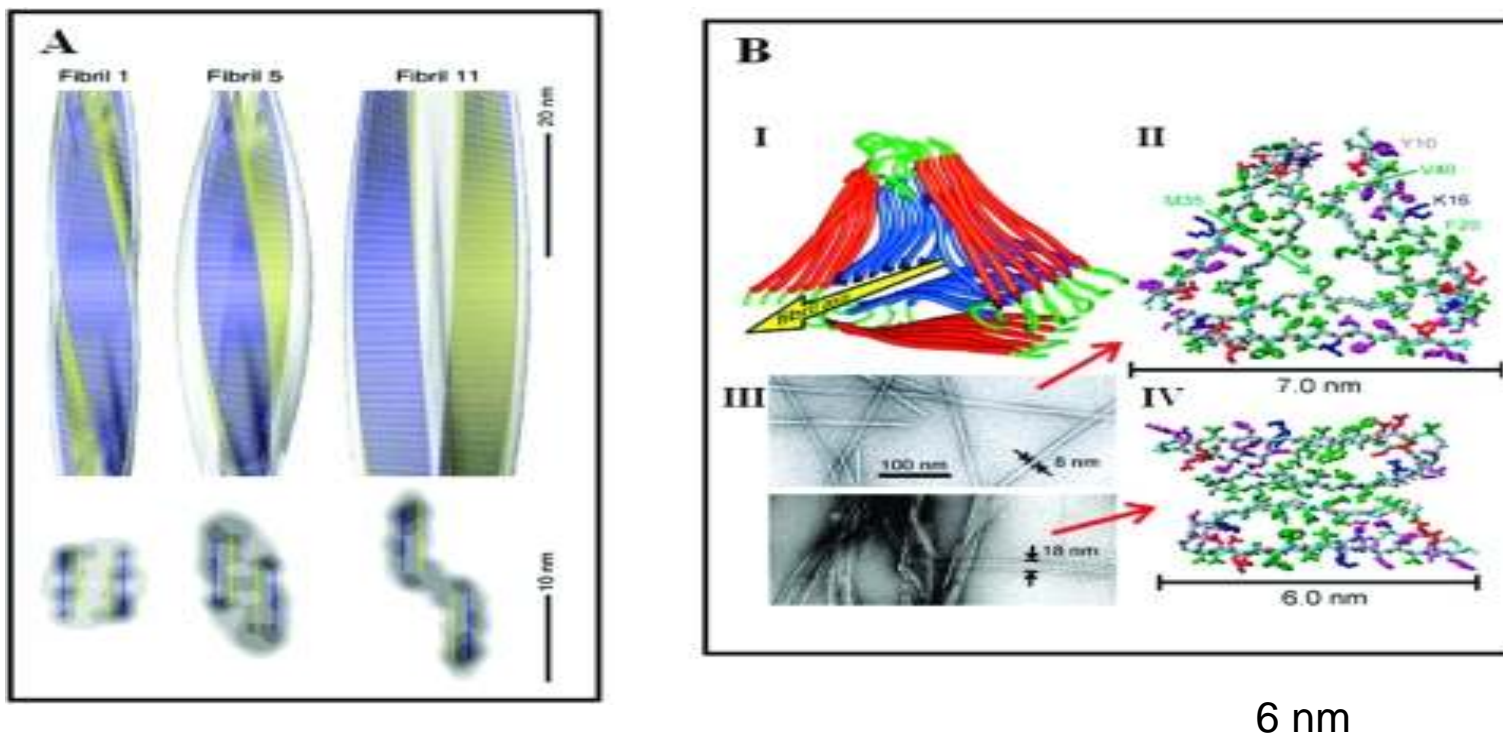
**Polymorphism in Alzheimer Abeta amyloid organization reflects conformational selection in a rugged energy landscape.**

[Miller Y](#), [Ma B](#), [Nussinov R](#).



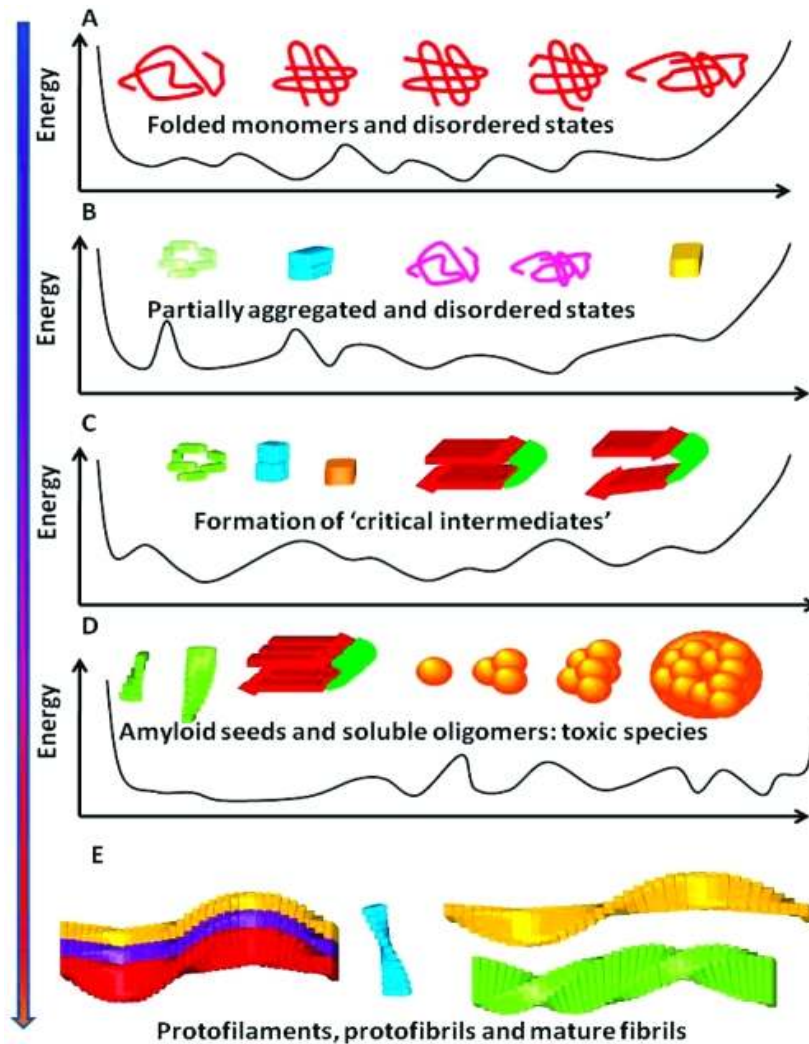
## [Chem Rev. 2010 August 11; 110\(8\): 4820–4838.](#)

Published online 2010 April 19. doi: 10.1021/cr900377t. <http://www.ncbi.nlm.nih.gov/pmc/articles/PMC2920034/figure/fig6/>



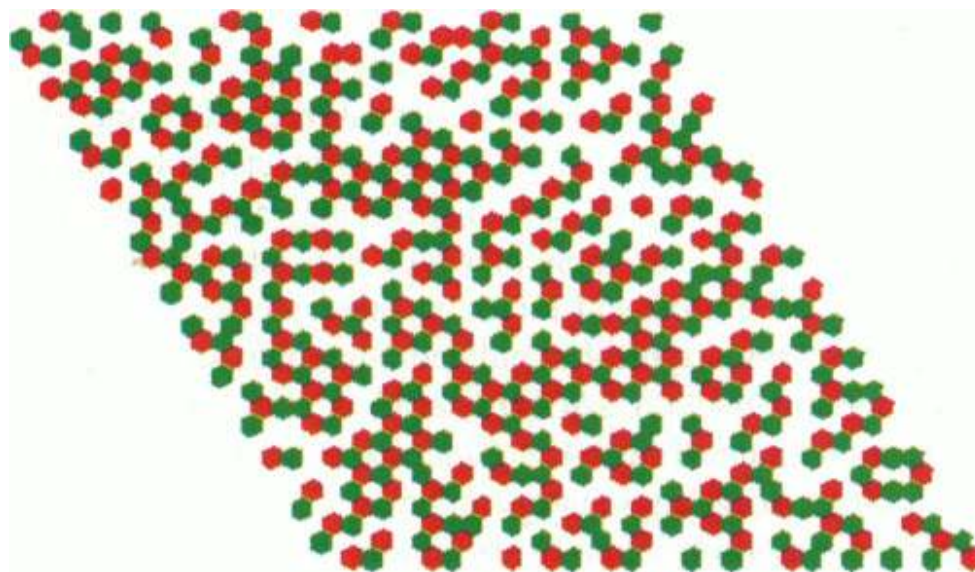
Polymorphism of the  $A\beta_{1-40}$  peptide based on different associations of the protofibrils. (A) A structural model of protofilament core topology of fibrils 1, 5, and 11, observed from Meinhardt et al. (73) Side view of the fibrils with two protofilament cores modeled into the density (top) and contoured density cross sections of the fibrils superimposed with two protofilament cores (bottom). Each protofilament core comprises a pair of two  $\beta$ -sheet regions: interface (yellow) and outside (blue). Reprinted with permission from ref (73). Copyright 2009 Elsevier. (B) Experiment-based structural models of  $A\beta_{9-40}$ . (I) A ribbon presentation of the lowest-energy model for fibrils with twisted morphology. (II) Atomic representation, viewed down the fibril axis. Hydrophobic, polar, negatively charged, and positively charged amino acid side-chains are green, magenta, red, and blue, respectively. Backbone nitrogen and carbonyl oxygen atoms are cyan and pink. (III) Comparison of twisted (upper) and striated ribbon (lower) fibril morphologies in negatively TEM images. (IV) Atomic representation of a model for striated ribbon fibrils developed previously by Petkova et al. (68,72) Reprinted with permission from ref (138). Copyright 2008 National Academy of Sciences.

**“Polymerization of A $\beta$  peptides involves continuous hierarchical redistributions of the polymorphic ensembles on a rugged energy landscape. For illustration, we present five aggregation phases starting from the native states and ending in the fibril forms.”**  
(loc.cit.)





# Monte-Carlo Simulations of Kinetically Irreversible Protein Aggregate Structure, such as A $\beta$



*“Typical simulated aggregate structure for type 1 monomers with  $\Delta\Delta G(H\phi, H\phi) = -5$  kcal/mol. The red and green hexagons represent the two unique rotational orientations of type 1 monomers. Adjacent red and green hexagons represent  $(H\phi, H\phi)$  interactions exclusively.”*

Source: Sugunakar Y. Patro and Todd M. Przybycien .1994. *Biophys. J.* **66**: 1274-1289.

<http://www.ncbi.nlm.nih.gov/pmc/articles/PMC1275849/pdf/biophysj00075-0011.pdf>

# Methods and models in neurodegenerative and systemic protein aggregation diseases

***Frontiers in Bioscience* 15, 373-396, January 1, 2010]**

**“Methods and models in neurodegenerative and systemic protein aggregation diseases” Ann-Christin Brorsson<sup>1</sup> et al 4.**

**Table 1.** *In vitro* and *in vivo* assays of protein aggregation behavior

## **Methods**

a. *In vitro* assays of protein aggregation behavior

In situ thioflavin T (polypeptide aggregation occurs in the presence of the dye) (38).

Provides a measure of beta-rich aggregates. This is a convenient method for generating multiple observations over a time course. Possible artifacts caused by the interaction of thioflavin T with aggregates.

Ex situ thioflavin T (aliquots are removed from the aggregation mixture and incubated with the dye) (28). Provides a measure of beta-rich aggregates. There are fewer concerns about dye binding artifacts.

More labor intensive. Disturbance caused by removing aliquots may cause artifacts.

Circular Dichroism

(CD) (33, 49-52).

Gives information about changes in secondary structure. No dye required.

# “Gene Therapy Reverses Symptoms of Parkinson's Disease”

## Source:

Claims from Weill Cornell Medical College / Recent Headline News-- **NEW YORK (March 17, 2011)** :

“RESULTS FROM THE FIRST SUCCESSFUL PHASE 2 CLINICAL TRIAL OF GENE THERAPY FOR PARKINSON'S **OR ANY NEUROLOGIC DISORDER.**”

“A gene therapy called NLX-P101 dramatically reduces movement impairment in Parkinson's patients, according to results of a Phase 2 study published today in the journal *Lancet Neurology*. The approach introduces a gene into the brain to **normalize chemical signaling.**”

Note: It has not been established that chemical signaling is the cause of all neurological disorders, thus the claim is unlikely to be extended to Alzheimer's

and other forms of dementia as an approved treatment!

Source location: [http://weill.cornell.edu/news/releases/wcmc/wcmc\\_2011/03\\_17\\_11.shtml](http://weill.cornell.edu/news/releases/wcmc/wcmc_2011/03_17_11.shtml)

# Extended Abstract of Parkinson's Gene Therapy News of March 17<sup>th</sup>, 2011

<<The study is the first successful randomized, double-blind clinical trial of a gene therapy for Parkinson's or any neurologic disorder, and it represents the culmination of 20 years of research by study co-authors Dr. Michael Kaplitt, Vice Chairman for Research in the Department of Neurological Surgery at Weill Cornell Medical College and a neurosurgeon at New York-Presbyterian Hospital/Weill Cornell Medical Center, and Dr. Matthew During, originally at Yale University, and now professor of Molecular Virology, Immunology and Medical Genetics, Neuroscience and Neurological Surgery at the Ohio State University.

(45) "*Patients who received NLX-P101 showed a significant reduction in the motor symptoms of Parkinson's, including tremor, rigidity and difficulty initiating movement,*" says Dr. Kaplitt, who pioneered the approach and helped design the clinical trial. "*This not only confirms the results of our Phase 1 trial performed at NewYork-Presbyterian/Weill Cornell but also represents a major milestone in the development of gene therapy for a wide range of neurological diseases.*" **AD ??**

**"This is great news for the 1.5 million Americans living with Parkinson's disease,"** adds Dr. During, who is the co-inventor, with Dr. Kaplitt, of the gene therapy procedure. **"Since this is also the first gene therapy study for a neurological disease to achieve success in a rigorous randomized, double-blind design compared with a sham group, this is also a crucial step forward toward finally bringing gene therapy into clinical practice for patients with debilitating brain disorders."**

Although medical therapy is usually effective for most symptoms of Parkinson's early in the disease, over time many patients become resistant to treatment or develop disabling side effects. An alternative treatment is electrical deep brain stimulation, which requires the implantation of permanent medical devices in the brain.>> (*loc.cit.*)

Exchanging the scalpel for gene therapy!

# NLX-P101 GENE THERAPY:

>>Gene therapy is the use of a gene to change the function of cells or organs to improve or prevent disease. To transfer genes into cells, an inert virus is used to deliver the gene into a target cell. In this case, the **glutamic acid decarboxylase** (GAD) gene was used because GAD makes a chemical called **GABA**, a major inhibitory neurotransmitter in the brain that **helps "quiet" excessive neuronal firing** related to Parkinson's disease. >>

**Note: this is the exact opposite of what happens in AD where the glutamic is actually used to slow down the AD progression!**

>>"In Parkinson's disease, not only do patients lose many dopamine-producing brain cells, but they also develop substantial reductions in the activity and amount of GABA in their brains. This causes a dysfunction in brain circuitry responsible for coordinating movement," explains Dr. During.

In the Phase 2 study, each patient in the experimental group received an infusion of the genetic material directly into their subthalamic nucleus, a key brain region involved in motor function. The GAD gene instructed cells in that area to begin making GABA neurotransmitters in order to re-establish the normal chemical balance which becomes dysfunctional within circuits that control movement.

While patients in the Phase 1 study only received the therapy on one side of their brain, **patients in the Phase 2 were infused on both sides**. And while the infusion happened entirely in the operating room in the previous phase, the current study made use of a novel delivery system conceived by Drs. Kaplitt and During that allowed for the infusion to take place outside of the OR — at the hospital bedside — something Dr. Kaplitt says makes for a more comfortable patient experience. **For more information, patients may call (866) NYP-NEWS.**

Drs. Kaplitt and During also designed the **sham surgery**, one of the most complex of its kind.

**The NLX-P101 gene therapy was pioneered by Neurologix, Inc.-- scientific founders Drs. Kaplitt and During >>**

**Let's hope that it's not all a sham!!**

## Additional, related details:

The Phase 2 study was funded by Neurologix Inc., of Fort Lee, N.J., which is developing the adeno-associated virus-borne GAD (AAV-GAD) agent and has licensed intellectual property rights to NLX-P101 gene therapy. **Drs. Kaplitt and Doring are co-founders of the company and remain paid consultants.** Additionally, **Dr. Kaplitt's father, Dr. Martin Kaplitt, is Chairman of the board of Neurologix, and as such has stock ownership and receives salary.** Leading the study were neurologists Dr. Andrew Feigin of the North Shore — LIJ Health System in Manhasset, N.Y., and Dr. Peter A. LeWitt of the Henry Ford Health System in West Bloomfield, Mich.

### **Additional co-authors include:**

Jason M. Schwalb from the [Henry Ford Health System](#), West Bloomfield Charter Township, Mich; Ali R. Rezai, Sandra K. Kostyk, Karen Thomas and Atom Sarkar from the Ohio State University College of Medicine, Columbus, Ohio; Maureen A. Leehey and Steven G. Ojemann from the University of Colorado School of Medicine, Aurora, Colo.; Alice W. Flaherty and Emad N. Eskandar from the Massachusetts General Hospital, Boston; Mustafa S. Siddiqui and Stephen B. Tatter from the Wake Forest University School of Medicine, Winston-Salem, N.C.; Kathleen L. Poston and Jaimie M. Henderson from the Stanford University School of Medicine, Stanford, Calif.; Roger M. Kurlan and Irene H. Richard from the University of Rochester School of Medicine, Rochester, N.Y.; Lori Van Meter from [PharmaNet Development Group](#), Princeton, N.J.; and **Christine V. Sapan from Neurologix Inc., Fort Lee, N.J.**

**No comment!**

# NEWYORK\*-PRESBYTERIAN HOSPITAL/WEILL CORNELL MEDICAL CENTER

❖ *“NewYork\*-Presbyterian Hospital/Weill Cornell Medical Center, located in New York City, is one of the leading academic medical centers in the world, comprising the teaching hospital NewYork-Presbyterian and Weill Cornell Medical College, the medical school of Cornell University. “*

❖ *“NewYork\*-Presbyterian/Weill Cornell provides state-of-the-art inpatient, ambulatory and preventive care in all areas of medicine, and is committed to excellence in patient care, education, research and community service.”*

**\*Not a misspelling!**

# Radioactivity and Radiation Dose Units

## 1. What units are used for measuring radioactivity?

Radioactivity or the strength of radioactive source is measured in units of becquerel (Bq): **1 Bq = 1 event of radiation emission per second.**

One becquerel is **an extremely small amount of radioactivity.**

[Commonly used multiples of the Bq unit are kBq (kilobecquerel), MBq (megabecquerel), and GBq (gigabecquerel). 1 kBq = 1000 Bq, 1 MBq = 1000 kBq, 1 GBq = 1000 MBq.]

An old and still popular unit of measuring radioactivity is the **curie (Ci)**. **1 Ci = 37 GBq = 37000 MBq.**]

**One curie is a large amount of radioactivity.** Commonly used subunits are mCi (millicurie),  $\mu$ Ci (microcurie), nCi (nanocurie), and pCi (picocurie). 1 Ci = 1000 mCi; 1 mCi = 1000  $\mu$ Ci; 1  $\mu$ Ci = 1000 nCi; 1 nCi = 1000 pCi.

Another useful conversion formula is: **1 Bq = 27 pCi, i.e., 1Bq = 27 pico-curies**

Becquerel (Bq) or Curie (Ci) are measures of **the rate (not energy) of radiation emission from a source.**

**2. Radiation Exposure Units:** X-ray and gamma-ray exposure unit is the **roentgen (R)\***. The roentgen (R) unit refers to the amount of ionization generated in 1cm<sup>3</sup> of air. In **SI** units, **1 R = 2.58×10<sup>-4</sup> C/kg = 1 esu/cm<sup>3</sup>**, and it generates about **2.08×10<sup>9</sup> ion** pairs/cm<sup>3</sup>, (from 1 esu  $\approx$  3.33564×10<sup>-10</sup> C and the standard atmosphere air density of  $\sim$ 1.293 kg/m<sup>3</sup>)

One roentgen of gamma- or x-ray exposure produces approximately **1 rad (0.01 gray) tissue dose.**

1 R exposure of tissue corresponds to  $\sim$ 10mSv (**1 rem**) absorbed, **equivalent dose** in the tissue. **1R  $\rightarrow$  10 mSv.**

**A 500 R (500rem) for 5 hours of X-rays or  $\gamma$ - exposure is lethal to humans  $\rightarrow$  5 Gy  $\rightarrow$  5Sv.**

**3. Radiation Dose:** The amount of energy absorbed per unit weight of the organ or tissue is called absorbed dose and is expressed in units of **gray (Gy) , 1Gy =100 rad.**

The equivalent dose is measured in **sievert (Sv)** units: see the next Table for differences between the effects of different types of radiation.

**\* “Strongly discouraged” to use it** by the [National Institute of Standards and Technology](#) style guide of NIST.



## Table 2. Recommended Radiation Weighting Factors

The dose in Sv is equal to “the absorbed dose” \* multiplied by a “radiation weighting factor”,  $W_R$  - shown in the following table.

[Prior to 1990, this weighting factor was referred to as a ‘Quality Factor’ (QF), and the old unit of “dose equivalent” or “dose” was the rem :  $1 \text{ Sv} = 100 \text{ rem}$  , or  $1 \text{ rem} = 10 \text{ mSv}$  .]

### Table of Recommended Radiation Weighting Factors:

Radiation Type and Energy range (for neutrons)	Radiation weighting factor, $W_R$
Gamma rays and X-rays	1
Beta particles	1
<b>Neutrons</b> , energy ranges	
< 10 keV	5
> 10 keV to 100 keV	10
> <b>100 keV to 2 MeV</b>	20
> 2 MeV to 20 MeV	10
> 20 MeV	5
<b>Alpha particles</b>	20

Source: [http://www.ccohs.ca/oshanswers/phys\\_agents/ionizing.html](http://www.ccohs.ca/oshanswers/phys_agents/ionizing.html)

\* The recommended TLV is average annual dose is < 50 mSv ! (5 rem !)

## **What are the limits of exposure to radiation?**

The Threshold Limit Values (TLVs) published by the ACGIH (American Conference of Governmental Industrial Hygienists) are used in many jurisdictions occupational exposure limits or guidelines:

**20 mSv** - TLV for average annual dose for radiation workers, averaged over five years

**1 mSv** - Recommended annual dose limit for general public (ICRP - International Commission on Radiological Protection).

## **What is the relationship between SI units and non-SI units?**

Table 3 shows SI units (International System of Units or *Système Internationale d'unités*), the corresponding non-SI units, their symbols, and the conversion factors.

# Table 3 . New SI vs. non-SI units

**Table 3**  
**Units of Radioactivity and Radiation Dose**

<b>Quantity</b>	<b>SI unit and symbol</b>	<b>Non-SI unit</b>	<b>Conversion factor</b>
Radioactivity	becquerel, Bq	curie, Ci	1 Ci = $3.7 \times 10^{10}$ Bq = 37 Gigabecquerels (GBq)  <b>1 Bq = 27 picocurie (pCi)</b>
Absorbed dose	gray, Gy	<b>rad</b>	<b>1 rad = 0.01 Gy</b>
"Dose" (Equivalent dose)	<b>sievert, Sv</b>	<b>rem</b>	1 rem = 0.01 Sv <b>1 rem = 10 mSv</b>

**Effective dose = Sum of [organ doses x tissue weighting factor,  $W_T$  ]**

Tissue weighting factors in Table 4 represent the relative sensitivity of organs for developing cancer.

**Table 4. Tissue Weighting Factors for Individual Tissues and Organs**

<b>Tissue or Organ</b>	<b>Tissue Weighting Factor (<math>W_T</math>)</b>
Gonads (testes or ovaries)	0.20
Red bone marrow	0.12
Colon	0.12
Lung	0.12
Stomach	0.12
Bladder	0.05
Breast	0.05
Liver	0.05
Oesophagus	0.05
Thyroid gland	0.05
Skin	0.01
Bone surfaces	0.01
Remainder**	0.05
Whole body	1.00

**\*\* The remainder is composed of the following additional tissues and organs: adrenal, brain, upper large intestine, small intestine, kidney, muscle, pancreas, spleen, thymus and uterus.**

# Radon Exposure at Home! --7,000 hours per year assumed

## Annual exposure from measured radon concentration

### (A) At home : assuming 7,000 hours spent indoors per year ?

$$1 \text{ Bq/m}^3 = 0.0156 \text{ mJ-h/m}^3$$

$$1 \text{ Bq/m}^3 = 0.0044 \text{ WLM}$$

$$1 \text{ WLM} = 4 \text{ mSv}$$

$$1 \text{ mJ-h/m}^3 = 1.1 \text{ mSv}$$

### (B) At work : assuming 2,000 hours work per year ?

$$1 \text{ Bq/m}^3 = 0.00445 \text{ mJ-h/m}^3 = 0.00126 \text{ WLM}$$

$$1 \text{ mJ-h/m}^3 = 1.4 \text{ mSv}$$

$$1 \text{ WLM} = 5 \text{ mSv}$$

$$1 \text{ WLM} = 3.54 \text{ mJ-h/m}^3 \quad 1 \text{ MBq-h/m}^3 = 2.22 \text{ mJ-h/m}^3$$

$$1 \text{ MBq-h/m}^3 = 0.628 \text{ WLM}$$

**Conversion of radon exposure units (equilibrium factor = 0.40)**

**Source:** ICRP Publication 65, Protection Against Radon at Home and at Work

# Radiation and Cancers

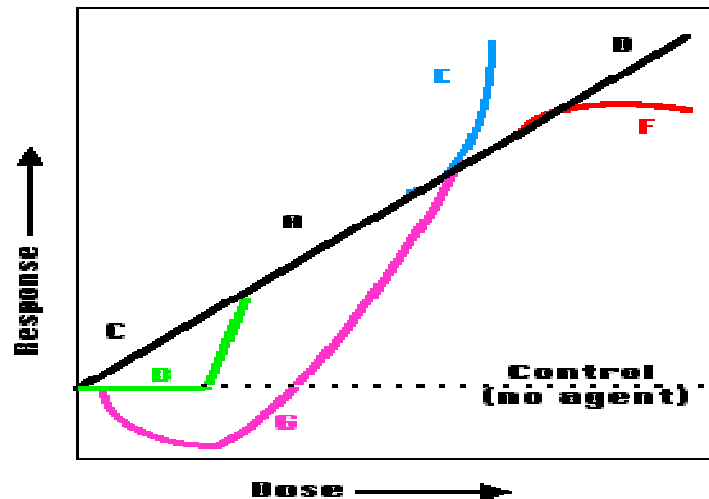
**Estimating Cancer Risks: Is there a safe dose of any mutagen or carcinogen?**

We live surrounded by [radiation](#) and by chemicals that cause [mutations](#) in test organisms (like [bacteria](#), yeast, and [mice](#)) cause an increase in the rate of cancers in experimental animals (rats and mice)

**Is there any safe dose for humans of these agents (which include oxygen!)?** The question is exceedingly difficult to answer and, I believe, at low doses, unanswerable. **Why?**

## Radiation and cancer

High doses of radiation cause cancer. Various studies, including excellent ones on the survivors of Hiroshima and Nagasaki, show that a **population** exposed to a dose of **100 millisieverts (mSv)** will have a measurable increase (about **1%**) in the incidence of cancer. **This is not small!** The total number of cancer deaths in the United States in 2009 was expected to exceed 560,000 from a population of 305 million (or ~ 0.2%) → → <20 mSv dose on average, or → 2 PET scans!



Source: This graph shows several theoretical dose-response relationships. There is considerable evidence that at moderate doses of a mutagen or [carcinogen](#), the response is linear (A). However, at very low doses of some chemicals, there may be a [threshold](#) below which the agent has no effect (B). The citizens of Colorado are exposed to background radiation of some 1.8 mSv per year; the figure for Massachusetts is only 1.02 mSv/year. 130mSv in Ramsar, Iran.

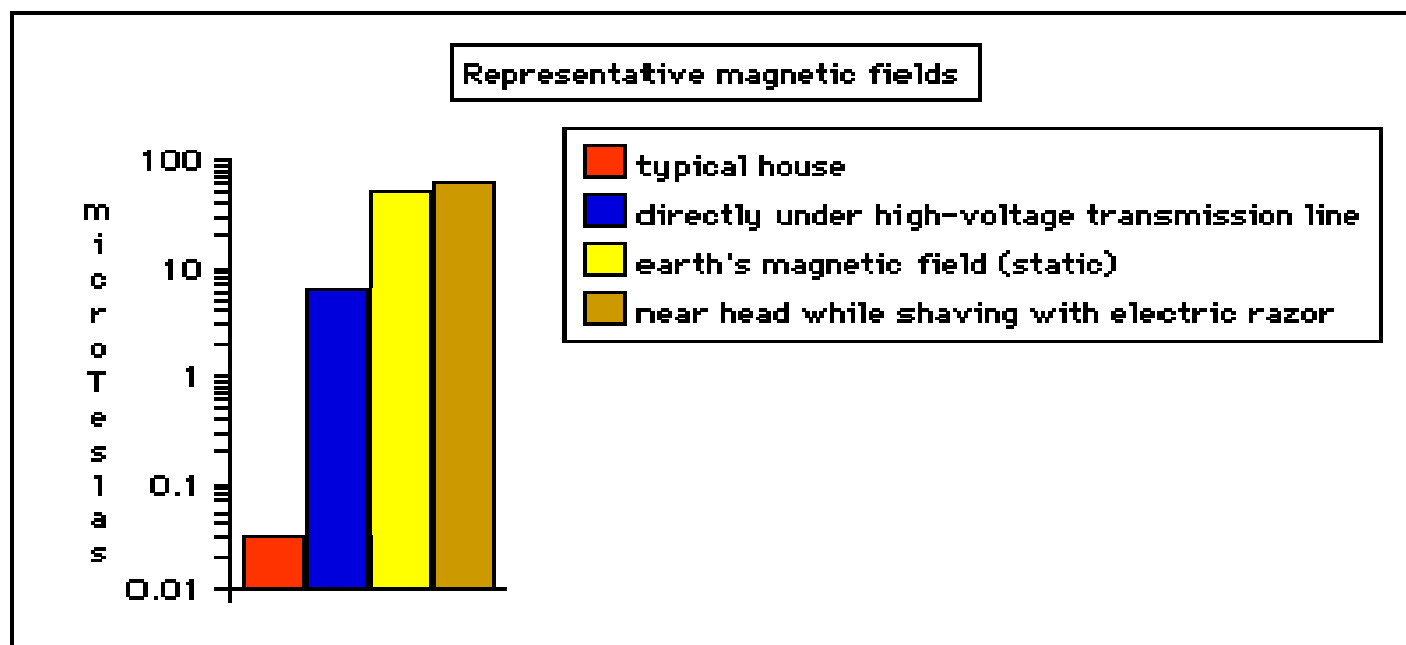
# Is There a Cancer-causing Dose Threshold ?

Many workers believe that for some agents, it is likely that **even the tiniest doses will have an effect** (C), but the population exposed must be large enough to observe it. This is called the **linear no-threshold** (LNT) model. Note that **even at zero dose, the line does not intercept the origin**. This is because even unexposed animals (including people) show a spontaneous level of response (e.g., tumors). There is also evidence that for some agents in some circumstances, increasing the dose (at relatively low levels) actually reduces the response below control levels (G). This phenomenon is called **hormesis**. **At very high doses, the rate of response may increase faster than the dose** (E) as, for example, the probability of a single cell suffering **two** mutations increases. On the other hand, very high doses may kill off damaged cells before they can develop into tumors (F).

## Radiation and cancer

**High doses of radiation cause cancer**. Various studies, including excellent ones on the survivors of Hiroshima and Nagasaki, show that a **population** exposed to a dose of **100 millisieverts** (**mSv**) will have a measurable increase (about **1%**) in the incidence of cancer. Note that the measurements are made on a population, **not on individuals**. We can never say that a particular individual exposed to a particular dose of radiation will develop cancer. The induction of cancer is a chance ("stochastic") event unlike the induction of **radiation sickness** which is completely predictable. The element of chance arises because cancer is an event that occurs in a single cell unlucky enough to suffer damage to several specific genes. **However, the energy needed to cause mutations is very low**. So if you expose a sufficiently large number of cells to even tiny doses of radiation, some cell is going to be unlucky. **How can we evaluate the risk?**

# Do 60 Hz High-Power Lines Cause Cancers in Children?



## The National Cancer Institute (NCI) Study:

On July 3, 1997, The New England Journal of Medicine published the largest and best study of the question (Martha S. Linet, et al, "*Residential Exposure to Magnetic Fields and **Acute Lymphoblastic Leukemia (ALL) in Children***"). **February 19<sup>th</sup>, 2011**

Their conclusion: "**Our results provide little support for the hypothesis that living in homes with high time-weighted average magnetic fields or in homes close to electrical transmission or distribution lines is related to the risk of childhood ALL**".

**"High-Power 60 Hz EM short transients could have effects ---not studied!—But , do such transients occur ?**



# General questions about patient's handling in PET scanning

FAQ replies to general questions about the patient handling are found at:

[http://rpop.iaea.org/RPOP/RPoP/Content/InformationFor/HealthProfessionals/6\\_OtherClinicalSpecialities/PETCTscan.htm#PETCT\\_FAQ01](http://rpop.iaea.org/RPOP/RPoP/Content/InformationFor/HealthProfessionals/6_OtherClinicalSpecialities/PETCTscan.htm#PETCT_FAQ01)

**Best answers are however provided only by qualified Nuclear Medicine specialists/ physicians !**

Actuaries will recognize this as a GM(1,3) function, familiar in the graduation of life tables (Forfar, McCutcheon & Wilkie, 1988), although as described below either  $F$  or  $G$  is set to zero. We found this flexible enough to give a good approximation to the ORs, and also suitable for extrapolating beyond age 90. The fitting procedure was as follows:

- (a) by considering the form of the OR, we set either  $F = 0$  (giving an exponential function) or  $G = 0$  (giving a bell-curve function), and set  $H$  equal to 0 or 1;
- (b) the best value of  $k_1$  or  $k_2$  was found, to the nearest integer, by inspection;

----

# New Marker Registration Possibilities

- $^{18}\text{F}$ -FDG PET compared with  $^{19}\text{F}$ FDG NMRI, even though the NMRI at fields used for clinical diagnosis has lower sensitivity than PET.
- This PET/NMRI registration or combination has the advantages of noninvasive NMRI combined with the selectivity of the FDG marker.